The productivity of two serial chemostats

Manel Dali-Youcef, Tewfik Sari

THE PRODUCTIVITY OF TWO SERIAL CHEMOSTATS

MANEL DALI-YOUCEF AND TEWFIK SARI

Abstract. This paper considers the production of biomass of two interconnected chemostats in serial with biomass mortality and a growth kinetic of the biomass described by an increasing function. A comparison is made with the productivity of a single chemostat with the same mortality rate and with volume equal to the sum of the volumes of the two chemostats. We determine the operating conditions under which the productivity of the serial configuration is greater than the productivity of the single chemostat. Moreover, the differences and similarities in the results corresponding to the case with mortality and the one without mortality, are highlighted. The mortality leads to surprising results where the productivity of a steady state where the bacteria are washed out in the first chemostat is greater than the one where the bacteria are present in both chemostats.

Contents

Date: November 24, 2021.

2010 *Mathematics Subject Classification.* Primary 34D20, 34H20, 65K10, 92C75.

Key words and phrases. chemostat, gradostat, mortality, bifurcations, global stability, operating diagram, biomass productivity.

1. Introduction

The mathematical model of the chemostat has received a great attention in the literature for many years (see for instance [6, 16] and literature cited inside). Several extensions of the original model of the chemostat, considering spatial heterogeneity, have been proposed to better cope reality. Discrete spatial representations, such as the gradostat model [16, 17], are a way to represent spatial heterogeneity. Serial configurations, are examples of gradostats, that have received a great interest in the literature in view of optimizing bioprocesses [4, 5, 7, 9, 10, 13, 15, 18]. A complete and deep analysis of the serial configuration of two chemostats was given in [2, 3], and the performance of the serial configuration were compared to those of the single chemostat, for three criteria : the *minimization of the output substrate concentration*, the *maximization of the biogas flow rate* and the *maximization of the productivity of the biomass*. In [2], it was proved that if a serial configuration is better than a single chemostat for one of these criteria, then it is also better for the other two criteria. More precisely, the serial chemostats have a smaller output substrate concentration than the single chemostat, if and only if it has a larger biogas flow rate (or productivity of the biomass). In fact, in [2], where the model does not consider mortality rate of the biomass, the biomass productivity and the biogas flow rate are given by the same expression. Hence, it is not surprising that the maximization of the biogas flow rate and the maximization of the productivity of the biomass are characterized by the same operating conditions. However, when the mortality of the biomass is introduced in the equations of the model, then the biomass productivity and the biogas flow rate are no longer given by the same expression. In the case where the mortality is included in the model, it was shown in [3] that the performance of the serial configuration, compared to a single chemostat, for the first and second criteria, lead to the same conclusions, i.e. the serial device has a smaller output substrate concentration than the single chemostat, if and only if it has a larger biogas flow rate. Characterizing the operating conditions for which the series device has a higher productivity than the single chemostat is a much more difficult problem. The aim of this article is to give the answer of this problem.

The paper is organized as follows. Section 2 describes the mathematical model corresponding to the serial configuration of two chemostats with mortality rate. The results on the existence and stability of the steady states obtained in [3] are outlined and the definition of the productivity of each steady state is given. The section ends with the comparison of these productivities with the one of the single chemostat, in case without mortality. This is an extension of former results obtained in [2]. Afterwards, Section 3 presents the comparison of these productivities with the one of the single chemostat, in the mortality case. Then, Section 4 considers the most efficient serial device when the two operating parameters (the input concentration of substrate and the dilution rate) are fixed. Section 5 provides illustrations of our results to the Monod growth function which is often used in the applications. However, our results are general and apply to a large class of growth functions, as illustrated in Appendix C. Finally, Section 6 contains a conclusion. Appendix A provides some results on the single chemostat that are used in this paper, while Appendix B gives the results on the existence and stability of the steady states of the model and its operating diagram. Some of the proofs are given in Section D.

2. The mathematical model

We consider two serial interconnected chemostats of volumes, V_1 and V_2. The substrate and the biomass concentrations are respectively denoted S_i and x_i, where $i = 1$ in the first chemostat and $i = 2$ in the second one. The input substrate concentration in the first chemostat is designated S^{in}, and Q is the flow rate, as shown in Figure 1.

The dilution rates in the chemostats are given by

$$D_1 := \frac{Q}{V_1} = \frac{D}{r}, \qquad D_2 := \frac{Q}{V_2} = \frac{D}{1-r}, \tag{1}$$

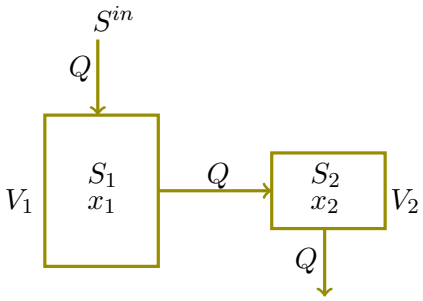

FIGURE 1. The serial configuration of two chemostats.

where $V = V_1 + V_2$ is the total volume, $r = V_1/V$ and $D = Q/V$. The mathematical model is given by the following equations:

$$\begin{aligned} \dot{S}_1 &= D_1(S^{in} - S_1) - x_1 \\ \dot{x}_1 &= -D_1 x_1 + f(S_1)x_1 - a x_1 \\ \dot{S}_2 &= D_2(S_1 - S_2) - f(S_2)x_2 \\ \dot{x}_2 &= D_2(x_1 - x_2) + f(S_2)x_2 - a x_2, \end{aligned} \tag{2}$$

where a is the mortality rate of the microorganism and f its specific growth rate. Note that equations (2) are not valid for $r = 0$ or $r = 1$. In these cases $V_1 = 0$ or $V_2 = 0$, and Figure 1 corresponds to a single chemostat of volume $V = V_1 + V_2$ and flow rate Q. Therefore, the dilution rate of this single chemostat is $D = Q/V$ and its mathematical equations are given by

$$\begin{aligned} \dot{S} &= D(S^{in} - S) - f(S)x \\ \dot{x} &= -Dx + f(S)x - ax \end{aligned} \tag{3}$$

where S and x denote respectively the substrate and the biomass concentration, see [6, 16]. We give in Appendix A the results on (3) that are necessary for the understanding of this paper. Note that singular perturbation theory shows that (3) is the reduced model associated with (2) in the limiting cases $r \to 0$ or $r \to 1$.

In (2), the input substrate concentration S^{in}, the volume V and the flow rate Q are assumed to be fixed, together with the ratio $r = V_1/V$. Therefore $D = Q/V$, S^{in} and r are the operating parameters in the model, since they can be easily chosen and manipulated by the experimenter of the device. Apart from these parameters, all other parameters have biological meaning and can be fitted using experimental data from real measurements of concentrations of micro-organisms and substrates. To provide the experimenter useful tools, the results on the behavior of the model are discussed with respect of the operating parameters and are describe using the so-called *operating diagram*. The operating diagram is the bifurcation diagram for which the values of the biological parameters are fixed. The various regions of the operating diagram reflect qualitatively different dynamics. The importance of the operating diagrams for bioreactors was emphasized in [11]. Since it is not easy to visualize regions in the three-dimensional operating parameters space, D and S^{in} are used as coordinates of the operating diagram, while r is kept constant. The effects of r are shown in a series of operating diagrams, see Figures 2, 7, 12, 13 and 16.

Our aim is to compare the productivity of (2) with the productivity of (3). We make the following assumption and notation:

Assumption 1. The function f is $\mathcal{C}^1$, with $f(0) = 0$ and $f'(S) > 0$ for all $S > 0$.

Notation 1. Let $\lambda : [0, m) \to \mathbb{R}^+$ be the inverse function of f, where $m := \sup_{S>0} f(S)$. For $D < m$, $S = \lambda(D)$ is called the break-even concentration. It is the unique solution of equation $f(S) = D$.

2.1. **The steady states and their stability.** The existence and stability of the steady states of (2) is studied in [3]. The system (2) can have up to three steady states:

- The washout steady state $E_0 = (S^{in}, 0, S^{in}, 0)$.

- The steady state $E_1 = (S^{in}, 0, \overline{S}_2, \overline{x}_2)$ of washout in the first chemostat but not in the second one.
- The steady state $E_2 = (S_1^*, x_1^*, S_2^*, x_2^*)$ of persistence of the species in both chemostats.

For the description of the steady state E_2 , we need to define the auxiliary function h given by:

$$h(S_2, S^{in}) = (D_2 + a)\frac{S_1^* - S_2}{\frac{D_1 S^{in} + a S_1^*}{D_1 + a} - S_2}, \quad \text{where} \quad S_1^* = \lambda\,(D_1 + a) \tag{4}$$

TABLE 1. The steady states of (2) and their conditions of existence and stability

The steady states E_1 and E_2 of (2)	
$E_1 = (S^{in}, 0, \overline{S}_2, \overline{x}_2)$	$\overline{S}_2 = \lambda\,(D_2 + a)$ and $\overline{x}_2 = \frac{D_2}{D_2+a}\left(S^{in} - \overline{S}_2\right)$
$E_2 = (S_1^*, x_1^*, S_2^*, x_2^*)$	$S_1^* = \lambda\,(D_1 + a)$, $x_1^* = \frac{D_1}{D_1+a}(S^{in} - S_1^*)$ S_2^* is the unique solution of equation $h(S_2, S^{in}) = f(S_2)$ and $x_2^* = \frac{D_2}{D_2+a}\,(x_1^* + S_1^* - S_2^*)$

	Existence condition	Stability condition
E_0	Always exists	$D_1 > f(S^{in}) - a$ and $D_2 > f(S^{in}) - a$
E_1	$D_2 < f(S^{in}) - a$	$D_1 > f(S^{in}) - a$
E_2	$D_1 < f(S^{in}) - a$	Stable if it exists

Theorem 1. [3] *Assume that Assumption 1 is satisfied. The components of the steady states of* (2) *and their conditions of existence and stability are given in Table 1.*

For the uniqueness of the solution of equation $h(S_2, S^{in}) = f(S_2)$ and other useful properties of the steady states, the reader is referred to Appendix B.

2.2. **Productivity of the biomass.** When a continuous culture system is viewed as a production process, its performance may be judged by the quantity of bacteria produced, which is called the productivity of biomass. The total output from a continuous culture unit in the steady state is equal to the product of flow-rate and concentration of organisms [8]. Therefore, for two serial interconnected chemostats, the production of biomass P_1 and P_2, corresponding respectively to the steady states E_1 and E_2, are given by

$$P_1 := Q\overline{x}_2 \quad \text{and} \quad P_2 := Qx_2^*, \tag{5}$$

where $\overline{x}_2$ and x_2^* are defined in Table 1. Using $Q = VD$, and the expressions of $\overline{x}_2$ and x_2^* given in Table 1, it is deduced that the productivities (5) depend on the operating parameters S^{in}, D and r and are given by the following formulas:

$$P_1(S^{in}, D, r) = \frac{VD^2}{D+(1-r)a}\left(S^{in} - \lambda\left(\frac{D}{1-r} + a\right)\right). \tag{6}$$

$$P_2(S^{in}, D, r) = \frac{VD^2}{D+(1-r)a}\left(\frac{D}{D+ra}(S^{in} - S_1^*) + S_1^* - S_2^*\right). \tag{7}$$

where $S_1^* = \lambda(D/r + a)$ and S_2^* is the unique solution of equation $f(S_2) = h(S_2, S^{in})$.

We recall that our aim is to compare the productivity of the serial configuration with the productivity of a single chemostat of total volume $V = V_1 + V_2$. The equations of the single chemostat are given by (3). The productivity of the single chemostat, denoted by P, is given by

$$P(S^{in}, D) = Qx^* = \frac{VD^2}{D+a}(S^{in} - \lambda(D + a)). \tag{8}$$

See Appendix A for details and complements.

2.3. **The case without mortality.** The productivities of the serial configuration (2), in the case where $a = 0$, are given by:

$$P_1(S^{in}, D, r) = VD\left(S^{in} - \lambda\left(\tfrac{D}{1-r}\right)\right), \tag{9}$$

$$P_2(S^{in}, D, r) = VD\left(S^{in} - S_2^*\right). \tag{10}$$

On the other hand, the productivity of the single chemostat (3), with $a = 0$, is

$$P(S^{in}, D) = VD\left(S^{in} - \lambda(D)\right). \tag{11}$$

We have the following results.

Proposition 1. *In the case $a = 0$, whenever the productivities are defined, we have*

$$P_1(S^{in}, D, r) < P(S^{in}, D), \tag{12}$$

$$P_1(S^{in}, D, r) < P_2(S^{in}, D, r), \tag{13}$$

$$P_2(S^{in}, D, r) > P(S^{in}, D) \Longleftrightarrow S^{in} > g_r(D), \tag{14}$$

where g_r is given by

$$g_r(D) = \lambda(D) + \tfrac{\lambda(D/r)-\lambda(D)}{1-r}. \tag{15}$$

Proof. We have $\lambda(D) < \lambda\left(D/(1-r)\right)$. Hence (12) holds, whenever P_1 and P are both defined. On the other hand, we have $S_2^* < \lambda\left(D/(1-r)\right)$, see Lemma 10 in the Appendix. Hence (13) holds, whenever P_1 and P_2 are both defined. Finally, (14) is a direct consequence of Theorem 2 in [2]. □

When the mortality is added in the model, the surprising result is that P_1 can be larger than P. Our aim is to give the operating conditions for which $P_1 > P$ and to extend (14) by giving the operating conditions for which $P_2 > P$. As a consequence we show that there are operating conditions for which $P_1 > P_2$, i.e. (13) is no longer true when $a > 0$.

3. Performance

3.1. **The performance at steady state E_1.** The productivity P_1 is given by (6). The following result gives the operating conditions for which $P_1 > P$.

Theorem 2. *Assume that Assumption 1 is satisfied. Let P_1 and P defined by* (6) *and* (8) *respectively. We have*

$$P_1(S^{in}, D, r) > P(S^{in}, D) \Longleftrightarrow S^{in} > p_1(D, r), \tag{16}$$

where p_1 is given by

$$p_1(D, r) := \lambda(D + a) + \tfrac{D+a}{ra}\left(\lambda\left(\tfrac{D}{1-r} + a\right) - \lambda(D + a)\right). \tag{17}$$

The equivalence (16) *holds when inequalities are replaced by equalities.*

Proof. From (8) and (6) we deduce that $P_1(S^{in}, D, r) > P(S^{in}, D)$ if and only if

$$\tfrac{1}{D+(1-r)a}\left(S^{in} - \lambda\left(\tfrac{D}{1-r} + a\right)\right) > \tfrac{1}{D+a}(S^{in} - \lambda(D + a)),$$

which is equivalent to $S^{in} > p_1(D, r)$, where p_1 is defined by (17). On the other hand, equality holds if and only if $S^{in} = p_1(D, r)$. □

Remark 1. The region where $S^{in} > p_1(D, r)$ disappears when $a \to 0$, which is consistent with (12). Indeed, from (17) one has $\lim_{a\to 0} p_1(D, r) = +\infty$.

Note that p_1 is defined on

$$\mathrm{dom}(p_1) := \{(D,r) : 0 \le D < m-a,\ 0 < r < 1 - D/(m-a)\}\,.$$

According to the Theorem 2, the curve Π_{r1} defined by

$$\Pi_{r1} = \left\{(S^{in}, D) : S^{in} = p_1(D,r)\right\} \tag{18}$$

is the set of operating conditions for which $P_1(S^{in}, D, r) = P(S^{in}, D)$. The result of Theorem 2 asserts that for all (S^{in}, D) at the right of the curve Π_{r1}, $P_1(S^{in}, D, r) > P(S^{in}, D)$. To have a better description of this set of operating conditions for which $P_1 > P$ we plot the curve Π_{r1} in the operating diagram, together with the curves

$$\Phi_{1-r} = \left\{(S^{in}, D) \in \mathbb{R}^2_+ : S^{in} = \lambda\big(\tfrac{D}{1-r} + a\big)\right\}, \tag{19}$$

$$\Phi_{r} = \left\{(S^{in}, D) \in \mathbb{R}^2_+ : S^{in} = \lambda\big(\tfrac{D}{r} + a\big)\right\}, \tag{20}$$

which determine the domain of existence and stability of E_1, see Appendix B.2. The Figure 2 shows a typical situation obtained with a specific Monod function. The red curves depicted in Figure 2 are the curves where $P_2 = P$ and will be described in the next section. The Figure 2 shows a situation where the curves Π_{r1} and Φ_r do not intersect. The case where these curves can intersect is investigated in Appendix C. Let us give more details on the relative positions of the curves Π_{r1}, Φ_r and Φ_{1-r}.

Proposition 2. *The curve Π_{r1} passes through point $(\lambda(a), 0)$, where Φ_r and Φ_{1-r} intersect. For $D > 0$, the curve Π_{r1} is at the right of the curve Φ_{1-r}. The curve Π_{r1} may intersect the curve Φ_r, with $D > 0$. If such an intersection exists then necessarily one has $0 < r < 1/2$ and D is a solution of equation*

$$(D+a)\lambda\left(\tfrac{D}{1-r} + a\right) - (D + a(1-r))\lambda\left(D + a\right) - ar\lambda\left(\tfrac{D}{r} + a\right) = 0. \tag{21}$$

Proof. From (17), it is seen that $p_1(0,r) = \lambda(a)$. Thus Π_{r1} passes through point $(\lambda(a), 0)$. From (17), it is deduced that

$$p_1(D,r) = \lambda\left(\tfrac{D}{1-r} + a\right) + \tfrac{D + a(1-r)}{ra}\left(\lambda\left(\tfrac{D}{1-r} + a\right) - \lambda\left(D + a\right)\right).$$

Hence, for $D > 0$ one has $p_1(D,r) > \lambda\left(\tfrac{D}{1-r} + a\right)$. From (19), it is deduced that Π_{r1} is at the right of Φ_{1-r}. If $r > 1/2$ then Φ_{1-r} is at the right of Φ_r, so that Π_{r1} cannot intersect Φ_r. From (18) and (20) it is deduced that the intersection points of Π_{r1} and Φ_r are the solutions of equation $p_1(D,r) = \lambda\left(D/r + a\right)$, which is equivalent to (21). □

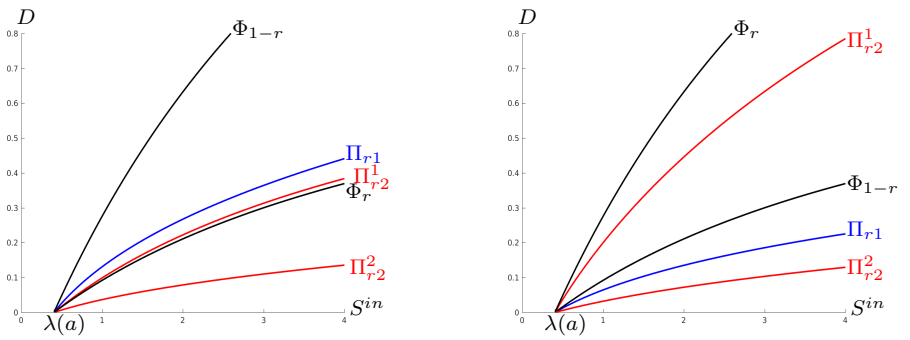

(a) $r = 0.25$ (b) $r = 0.75$

FIGURE 2. The operating diagram showing the curves Π_{r1} (in blue), Φ_{1-r} and Φ_r (in black), and Π^1_{r2} and Π^2_{r2} (in red), defined respectively by (18), (19), (20), (31) and (32). The figure is done using $f(S) = 4S/(5+S)$ and $a = 0.3$.

Note that the steady state E_1 may have a greater productivity than the single chemostat and be either stable or unstable. If the operating condition (S^{in}, D) is chosen at the right of Π_{r1} and at the left of Φ_r in Figure 2(a), then E_1 exists and is stable, and satisfies $P_1 > P$. In this case E_2 does not exist. On the other hand, if (S^{in}, D) is chosen at the right of Φ_r in Figure 2(a), then E_1 exists and is unstable, and satisfies $P_1 > P$. In this case E_2 exists (and is stable). In Figure 2(b), E_1 is unstable whenever it exists and, for (S^{in}, D) at the right of Π_{r1} in Figure 2(b), one has $P_1 > P$.

For the operating conditions, for which $P_1 > P$, from the practical point of view, one should simply consider a tank of volume $(1-r)V$ and obtain a productivity which is higher than the productivity of the tank of volume V. The surprising result is that the productivity of the tank of volume V is smaller than the productivity of the tank of volume $(1-r)V$. This surprising result is due to the mortality in the chemostat. If there is no mortality, then $P_1(S^{in}, D, r) < P(S^{in}, D)$ for any S^{in}, D and r, for which P_1 and P are defined, as shown by (12) in Proposition 1.

3.2. **The performance at steady state E_2.** Our aim in this section is to compare the productivity P_2 of E_2 and the productivity P of the single chemostat. The productivity P_2 is given by (7). We need the following notations:

$$\alpha = \frac{a^2 r(1-r)}{(D+a)(D+ra)}, \quad \beta = \frac{ra}{D+ra} S_1^* + \frac{D+(1-r)a}{D+a} \lambda(D+a), \tag{22}$$

$$A = -\alpha S^{in} + \beta, \tag{23}$$

$$h_2(S_2) = h\left(S_2, \frac{\beta - S_2}{\alpha}\right), \tag{24}$$

$$h_1(S^{in}) = h(-\alpha S^{in} + \beta, S^{in}), \quad f_1(S^{in}) = f(-\alpha S^{in} + \beta). \tag{25}$$

Lemma 1. *Let P_2 and P defined respectively by* (7) *and* (8)*. The following conditions are equivalent.*

(1) $P_2(S^{in}, D, r) > P(S^{in}, D)$.
(2) $S_2^* < A$.
(3) $h_2(A) < f(A)$.
(4) $h_1(S^{in}) < f_1(S^{in})$.

These conditions are also equivalent if inequalities are replaced by equalities.

Proof. From (7) and (8) it is deduced that $P_2(S^{in}, D, r) > P(S^{in}, D)$ if and only if

$$\frac{1}{D+(1-r)a}\left(\frac{D}{D+ra}(S^{in} - S_1^*) + S_1^* - S_2^*\right) > \frac{1}{D+a}(S^{in} - \lambda(D+a)),$$

which is equivalent to $S_2^* < A$, where A is defined by (23). This proves the equivalence of the conditions (1) and (2) in the lemma. Recall that S_2^* is the unique solution of equation $h(S_2, S^{in}) = f(S_2)$, see Table 1. Since $S_2 \mapsto f(S_2)$ is increasing and $S_2 \mapsto h(S_2, S^{in})$ is decreasing then, the condition (2) is equivalent to

$$h(A, S^{in}) < f(A). \tag{26}$$

Replacing S^{in} by $S^{in} = (\beta - A)/\alpha$ it is seen that the condition (26) is equivalent to $h_2(A) < f(A)$, where h_2 is defined by (24). This proves the equivalence of the conditions (2) and (3). Similarly, replacing A by $A = -\alpha S^{in} + \beta$, it is seen that the condition (26) is equivalent to $h_1(S^{in}) < f_1(S^{in})$, where h_1 and f_1 are defined by (25). This proves the equivalence of the conditions (2) and (4). The proof of the equivalence of the conditions when inequalities are replaced by equalities is the same. □

Therefore we must solve the equation $h_2(S_2) = f(S_2)$ where h_2 is defined by (24). From (4), it is seen that the function h is given by

$$h(S_2, S^{in}) := \frac{D+(1-r)a}{1-r} \frac{S_1^* - S_2}{\frac{DS^{in} + raS_1^*}{D+ra} - S_2}. \tag{27}$$

Using the expressions of α and β given by (22), straightforward computations give

$$h_2(S_2) = \frac{ra^2}{D+ra} \frac{S_1^* - S_2}{\sigma - S_2}, \quad \text{with} \quad \sigma := \frac{D\lambda(D+a) + raS_1^*}{D+ra}. \tag{28}$$

The graph of h_2 is an increasing hyperbola with $y = ra^2/(D+ra)$ as horizontal asymptote and $S_2 = \sigma$ as vertical asymptote. Let us show that this graph intersect the graph of the increasing function f in at least two points, see Figure 3(a).

Lemma 2. *The equation $h_2(S_2) = f(S_2)$ has two solutions $S_2^1(D,r)$ and $S_2^2(D,r)$, such that $0 < S_2^2(D,r) < \lambda(D+a) < S_2^1(D,r) < \sigma$. Moreover, if $0 \leq S_2 < S_2^2(D,r)$ or $S_2^1(D,r) < S_2 < \sigma$, then we have $h_2(S_2) > f(S_2)$. In addition, assuming that there is no other solution, then we have $h_2(S_2) < f(S_2)$ if and only if $S_2^2(D,r) < S_2 < S_2^1(D,r)$.*

Proof. The function $H(S_2) := h_2(S_2) - f(S_2)$ is defined for $0 < S_2 < \sigma$. One has $H(\sigma) = +\infty$ and

$$H(0) = \frac{ra^2 S_1^*}{D\lambda(D+a)+raS_1^*} > 0.$$

Notice that $\lambda(D+a) < \sigma$ because σ is a convex combination of $\lambda(D+a)$ and S_1^*, and $S_1^* > \lambda(D+a)$. Let us calculate $H(\lambda(D+a))$. From $h_2(\lambda(D+a)) = a$ and $f(\lambda(D+a)) = D+a$ it is deduced that $H(\lambda(D+a)) = -D$ which is negative. Consequently, using the Intermediate Value Theorem, one deduces that equation $H(S_2) = 0$ admits a smallest solution, denoted by $S_2^2(D,r)$, in the interval $(0, \lambda(D+a))$, and a largest one, denoted by $S_2^1(D,r)$, in the interval $(\lambda(D+a), \sigma)$. Therefore $h_2(S_2) > f(S_2)$ for $S_2 < S_2^2(D,r)$ or $S_2 > S_2^1(D,r)$. If there is no other zero in the interval $(S_2^2(D,r), S_2^1(D,r))$ then the condition $h_2(S_2) < f(S_2)$ is equivalent to $S_2^2(D,r) < S_2 < S_2^1(D,r)$, see Figure 3 (a). □

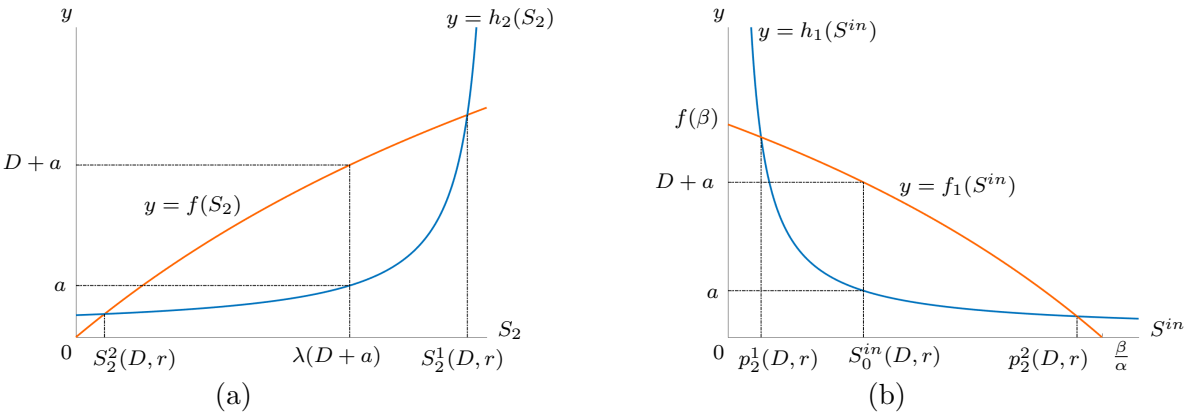

FIGURE 3. (a): The solutions $S_2^1(D,r)$ and $S_2^2(D,r)$ of $h_2(S_2) = f(S_2)$. (b): The solutions $p_2^1(D,r)$ and $p_2^2(D,r)$ of $h_1(S^{in}) = f_1(S^{in})$.

We make the following assumption, which is satisfied by any concave growth function but also by any Hill function, see Section C.

Assumption 2. Equation $h_2(S_2) = f(S_2)$ admits only two solutions.

Notation 2. Let $S_2^1(D,r)$ and $S_2^2(D,r)$ be the solutions of equation $h_2(S_2) = f(S_2)$, such that $S_2^2(D,r) < \lambda(D+a) < S_2^1(D,r)$.

Lemma 3. *Assume that Assumption 2 holds. Equation $h_1(S^{in}) = f_1(S^{in})$, where h_1 and f_1 are defined by (25) admits two solutions $p_2^1(D,r)$ and $p_2^2(D,r)$ defined for $0 < r < 1$ and $0 \leq D < r(m-a)$, such that $\lambda(D+a) < p_2^1(D,r) < S_0^{in}(D,r) < p_2^2(D,r) < \beta/\alpha$, where α and β are given by (22) and*

$$S_0^{in}(D,r) := \frac{\beta - \lambda(D+a)}{\alpha} = \lambda\left(\frac{D}{r} + a\right) + \frac{D+ra}{a(1-r)}\left(\lambda\left(\frac{D}{r} + a\right) - \lambda(D+a)\right).$$

Moreover we have $h_1(S^{in}) < f_1(S^{in})$ if and only if $p_2^1(D,r) < S^{in} < p_2^2(D,r)$.

Proof. According to Lemma 2, $S_2^1(D,r)$ and $S_2^2(D,r)$ defined in Notation 2 satisfy the condition: $h_2(S_2) < f(S_2)$ if and only if $S_2^2(D,r) < S_2 < S_2^1(D,r)$. Let p_2^1 and p_2^2 be defined by

$$p_2^1(D,r) = \tfrac{\beta - S_2^1(D,r)}{\alpha} \quad \text{and} \quad p_2^2(D,r) = \tfrac{\beta - S_2^2(D,r)}{\alpha}. \tag{29}$$

From the condition $0 < S_2^2(D,r) < \lambda(D+a) < S_2^1(D,r) < \sigma$, it is deduced that

$$\lambda(D+a) < p_2^1(D,r) < S_0^{in}(D,r) < p_2^2(D,r) < \beta/\alpha.$$

We deduce that the condition $h_1(S^{in}) < f_1(S^{in})$ is equivalent to $p_2^1(D,r) < S^{in} < p_2^2(D,r)$, see Figure 3 ($b$). □

The following result gives the operating conditions for which $P_2 > P$.

Theorem 3. *Assume that Assumptions 1 and 2 hold. Let P_2 and P be defined by* (7) *and* (8) *respectively. We have*

$$P_2(S^{in},D,r) > P(S^{in},D) \Longleftrightarrow \max(\lambda(D/r+a), p_2^1(D,r)) < S^{in} < p_2^2(D,r), \tag{30}$$

where $p_2^1(D,r)$ and $p_2^2(D,r)$ are given in Lemma 3. If $p_2^1(D,r) \geq \lambda(D/r+a)$, then, the equality $P_2(S^{in},D,r) = P(S^{in},D)$ holds if and only if $S^{in} = p_2^1(D,r)$ or $S^{in} = p_2^2(D,r)$.

Proof. The result is a consequence of Lemmas 1 and 3. □

According to the Theorem 3, the set $\Pi_{r2} = \Pi_{r2}^1 \cup \Pi_{r2}^2$, where Π_{r2}^1 and Π_{r2}^2 curves are given by

$$\Pi_{r2}^1 = \left\{(S^{in},D) : S^{in} = p_2^1(D,r)\right\}, \tag{31}$$

$$\Pi_{r2}^2 = \left\{(S^{in},D) : S^{in} = p_2^2(D,r)\right\}, \tag{32}$$

is the set of operating conditions for which $P_2(S^{in},D,r) = P(S^{in},D)$. The result of Theorem 3 asserts that for all (S^{in},D) at the right of Π_{r2}^1 and the left of Π_{r2}^2, then if E_2 exists, we have $P_2(S^{in},D,r) > P(S^{in},D)$.

To have a better description of this set of operating conditions for which $P_2 > P$ we plot the curve Π_{r2}^1 and Π_{r2}^2 in the operating diagram, together with the curves Π_{r1}, Φ_{1-r} and Φ_r, see Figure 2. Before analyzing the features depicted by this example, let us give some details on the relative positions of curves Π_{r2}^1, Π_{r2}^2 and Φ_r in the general case.

Proposition 3. *The curves Π_{r2}^1 and Π_{r2}^2, pass through point $(\lambda(a),0)$, where Φ_r and Φ_{1-r} intersect. For $D>0$, the curve Π_{r2}^2 is at the right of the curve Φ_r. The curve Π_{r2}^1 may intersect the curve Φ_r, with $D>0$. If such an intersection exists then necessarily one has $0<r<1/2$ and $\Phi_r \cap \Pi_{r2}^1 = \Phi_r \cap \Pi_{r1}$.*

Proof. Note that if $D=0$ then equation $h(S_2) = f(S_2)$ has the unique solution $S_2 = \lambda(a)$, since $h_2(\lambda(a)) = f(\lambda(a)) = a$, see Figure 3(a). Therefore, $S_2^1(0,r) = S_2^2(0,r) = \lambda(a)$. Hence, using the fact that if $D=0$ we have $\alpha = 1-r$ and $\beta = (2-r)\lambda(a)$, from (29), it is deduced that

$$p_2^1(0,r) = p_2^2(0,r) = \tfrac{\beta-\lambda(a)}{\alpha} = \tfrac{(2-r)\lambda(a)-\lambda(a)}{1-r} = \lambda(a).$$

This proves that Π_{r2}^1 and Π_{r2}^2, pass through point $(\lambda(a),0)$. From the definition of S_0^{in} in Lemma 3, it is seen that $p_2^2(D,r) > S_0^{in}(D,r) > \lambda\left(\frac{D}{r}+a\right)$. Therefore from (20) and (32) we deduce that for $D>0$, Π_{r2}^2 is at the right of Φ_r. On the other hand, the curve Φ_r corresponds to a transcritical bifurcation of E_1 and E_2, see Remark 1 in [3]. Hence, on this curve, one has $E_1 = E_2$, so that $P_1 = P_2$, which proves that $\Phi_r \cap \Pi_{r1} = \Phi_r \cap \Pi_{r2}^1$. □

Remark 2. If (S^{in},D) is chosen at the right of Π_{r2}^2, then E_2 exists (since (S^{in},D) is necessarily at the right of Φ_r), and satisfies $P_2 < P$. If (S^{in},D) is chosen at the right of Φ_r and between curves Π_{r2}^1 and Π_{r2}^2, then E_2 exists and satisfies $P_2 > P$.

Therefore, for (S^{in},D) at the right of Φ_r and at the left of Π_{r2}^2 in Figure 2(a), one has $P_2 > P$. For (S^{in},D) at the right of Π_{r2}^1 and at the left of Π_{r2}^2 in Figure 2(b), one has $P_2 > P$. Similarly, for (S^{in},D) at the right of Π_{r2}^2 in Figure 2, one has $P_2 < P$. The surprising result is that the productivity P_2 may be smaller than the productivity P_1. Indeed, suppose that point (S^{in},D) is

located at the right of Π^2_{r2} in Figure 2, then its lies also at the right of Π_{r1}, and, from Theorems 2 and 3, it is deduced that

$$P_2(S^{in}, D, r) < P(S^{in}, D) < P_1(S^{in}, D, r).$$

This result is surprising since, the productivity P_1 corresponds to the steady state E_1, where species x_1 is washed out in the first tank, is greater than the productivity P_2 of the steady state E_2 of coexistence. This surprising result is due to the mortality in the chemostat. If there is no mortality, then $P_1(S^{in}, D, r) < P_2(S^{in}, D, r)$ for any S^{in}, D and r, for which P_1 and P_2 are both defined, as shown by (13) in Proposition 1. Let us show that the result of Theorem 3 extends (14) in Proposition 1. We have the following result:

Proposition 4. *Let p_2^1 and p_2^2 defined as in Lemma 3. We have*

$$\lim_{a\to 0} p_2^2(D, r) = +\infty, \qquad \lim_{a\to 0} p_2^1(D, r) = g_r(D),$$

where g_r is defined by (15).

Proof. Straightforward computations give

$$h_1(S^{in}) = \eta + \tfrac{\rho}{S^{in}-\lambda(D+a)}, \quad \text{with} \quad \eta = \tfrac{ra^2}{D+ra}, \quad \rho = \tfrac{D(D+a)}{D+ra}\,\tfrac{\lambda(D/r+a)-\lambda(D+a)}{1-r}. \tag{33}$$

Recall that p_2^1 and p_2^2 are the solutions of the equation $f_1(S^{in}) = h_1(S^{in})$, where $f_1(S^{in})$ is given by $f_1(S^{in}) = f(-\alpha S^{in} + \beta)$, see Lemma 3. Note that the graph of h_1 is a decreasing hyperbola with $S^{in} = \lambda(D+a)$ as vertical asymptote and $y = \eta$ as horizontal asymptote, while $y = f_1(S^{in})$ is a decreasing function from $f_1(0) = f(\beta)$ to $f_1(\beta/\alpha) = 0$, see Figure 3(b). Using the limits

$$\lim_{a\to 0} \alpha = 0, \quad \lim_{a\to 0} \beta = \lambda(D), \quad \lim_{a\to 0} \eta = 0, \quad \lim_{a\to 0} \rho = D\tfrac{\lambda(D/r)-\lambda(D)}{1-r},$$

it is seen that the graph of $y = f_1(S^{in})$ converges toward the horizontal line $y = f(\lambda(D)) = D$, while the graph of $y = h_1(S^{in})$ converges toward the hyperbola

$$y = \tfrac{D}{1-r}\tfrac{\lambda(D/r)-\lambda(D)}{S^{in}-\lambda(D)}.$$

Therefore, $p_2^2(D, r)$, the largest solution of equation $f_1(S^{in}) = h_1(S^{in})$ converges toward $+\infty$ and $p_2^1(D, r)$, the smallest solution, converges toward the solution of equation

$$D = \tfrac{D}{1-r}\tfrac{\lambda(D/r)-\lambda(D)}{S^{in}-\lambda(D)}.$$

The solution of this equation is $S^{in} = g_r(D)$, where g_r is given by (15). Therefore, $p_2^1(D, r)$ converges toward $g_r(D)$. □

Remark 3. When $a \to 0$, the region between the curves Π^1_{r2} and Π^2_{r2}, where $P_2(S^{in}, D, r) > P(S^{in}, D)$ tends towards the region defined by $S^{in} > g_r(D)$, which is consistent with (14) in Proposition 1.

3.3. **The behavior of the productivity with respect of the dilution rate.** To give a better understanding of the behavior of the productivity we fix $S^{in} > \lambda(a)$ and $r \in (0, 1)$ and we describe the functions $D \mapsto P_1(S^{in}, D, r)$ and $D \mapsto P_2(S^{in}, D, r)$. We compare them with the function $D \mapsto P(S^{in}, D)$.

Lemma 4. *Let $S^{in} > \lambda(a)$ and $r \in (0, 1)$ be fixed. The function $D \mapsto P_1(S^{in}, D, r)$ is defined for $D \in \big[0, \delta_1(S^{in}, r)\big]$, where $\delta_1(S^{in}, r) = (1 - r)(f(S^{in}) - a)$. It satisfies*

$$P_1(S^{in}, 0, r) = P_1(S^{in}, \delta_1(S^{in}, r), r) = 0.$$

The function $D \mapsto P_2(S^{in}, D, r)$ is defined for $D \in \big[0, \delta_2(S^{in}, r)\big]$, where $\delta_2(S^{in}, r) = r(f(S^{in}) - a)$. It satisfies $P_2(S^{in}, 0, r) = 0$, and

$$P_2(S^{in}, \delta_2(S^{in}, r), r) = \begin{cases} P_1(S^{in}, \delta_2(S^{in}, r), r) & \text{if} \quad r \le 1/2, \\ 0 & \text{if} \quad r \ge 1/2. \end{cases}$$

Proof. The productivity P_1 is defined where the steady state E_1 is also defined. Therefore P_1 is defined if and only if $0 \leq D \leq (1-r)(f(S^{in})-a)$. The productivity P_2 is defined where the steady state E_2 is also defined. That is to say, P_2 is defined if and only if $0 \leq D \leq r(f(S^{in})-a)$. From the definitions (6) and (7) we have

$$P_1(S^{in},0,r) = P_2(S^{in},0,r) = 0.$$

For $D = \delta_1(S^{in},r)$, there is a transcritical bifurcation of E_1 and E_0, see Remark 1 in [3]. Therefore $P_1(S^{in},\delta_1(S^{in},r),r) = 0$. Similarly, for $D = \delta_2(S^{in},r)$, there is a transcritical bifurcation of E_2 and E_0, if $r \geq 1/2$, and a transcritical bifurcation of E_2 and E_1, if $r \leq 1/2$. This gives the value of P_2 for $D = \delta_2(S^{in},r)$. □

Note that $p_1(0,r) = \lambda(a)$ and, since $\lim_{D\to m} \lambda(D) = +\infty$, we have

$$\lim_{D\to(1-r)(m-a)} p_1(D,r) = +\infty.$$

Therefore, if the function $D \mapsto p_1(D,r)$ is increasing, then it admits an inverse function $S^{in} \mapsto d_1(S^{in},r)$, and the equation $S^{in} = p_1(D,r)$ is equivalent to the equation $D = d_1(S^{in},r)$. More precisely, we add the following assumption which is satisfied by any concave growth function but also by any Hill function, see Appendix C.

Assumption 3. For every $r \in (0,1)$, the function $D \mapsto p_1(D,r)$ is increasing.

Notation 3. Let $S^{in} \mapsto d_1(S^{in},r)$ be the inverse function of the function $D \mapsto p_1(D,r)$. It is defined for $S^{in} \geq \lambda(a)$.

Theorem 4. *Assume that Assumptions 1 and 3 are satisfied. Then $P_1(S^{in},D,r) > P(S^{in},D)$ if and only if $0 < D < d_1(S^{in},r)$.*

Proof. Let $r \in (0,1)$. The function $D \mapsto p_1(D,r)$ is increasing. Therefore, the property $0 < D < d_1(S^{in},r)$ is satisfied if and only if $0 < p_1(D,r) < S^{in}$. According to Theorem 2, this is equivalent to $P_1(S^{in},D,r) > P(S^{in},D)$. □

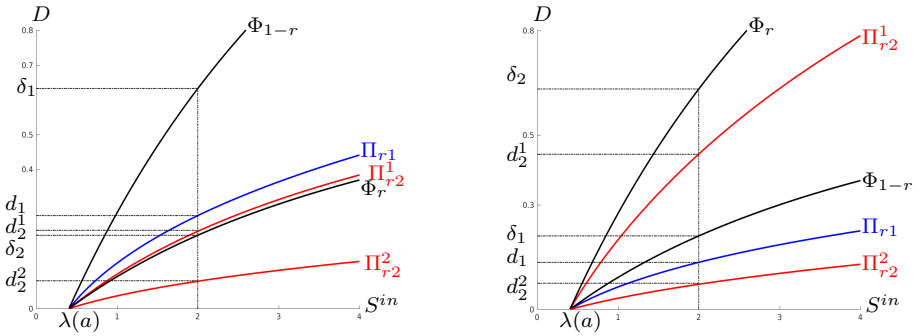

(a) $r = 0.25$ (b) $r = 0.75$

FIGURE 4. For $S^{in} = 2$, the depiction of $\delta_1(S^{in},r)$ and $\delta_2(S^{in},r)$, defined in Lemma 4, $d_1(S^{in},r)$ defined in Notation 3, and $d_2^1(S^{in},r)$, $d_2^2(S^{in},r)$, defined in Notation 4. The biological parameters are as in Figure 2.

Lemma 5. *Let $r \in (0,1)$. The functions $D \mapsto p_2^1(D,r)$ and $D \mapsto p_2^2(D,r)$ are defined for $D \in [0, r(m-a))$ and satisfy $p_2^1(0,r) = p_2^2(0,r) = \lambda(a)$ and*

$$\lim_{D\to r(m-a)} p_2^1(D,r) = \lim_{D\to r(m-a)} p_2^2(D,r) = +\infty.$$

Proof. The functions $D \mapsto p_2^1(D,r)$ and $D \mapsto p_2^2(D,r)$ are defined where the steady state E_2 is defined, i.e. for $D/r + a < m$, which is equivalent to $D < r(m-a)$. From Lemma 3, the

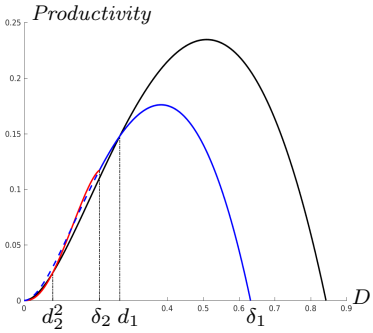

(a) $r = 0.25$, $S^{in} = 2$

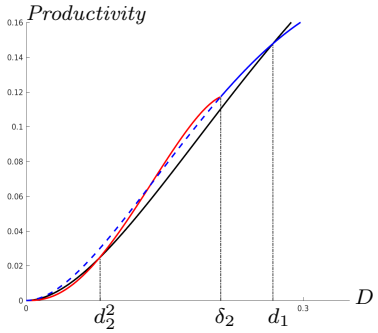

(b) Zoom of (a) showing d_1, δ_2 and d_2^2

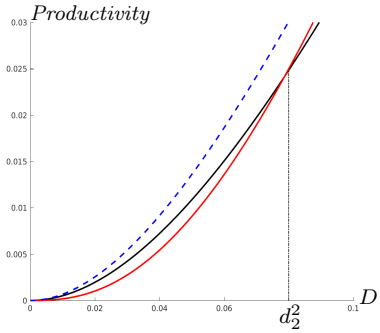

(c) Zoom of (b) showing d_2^2

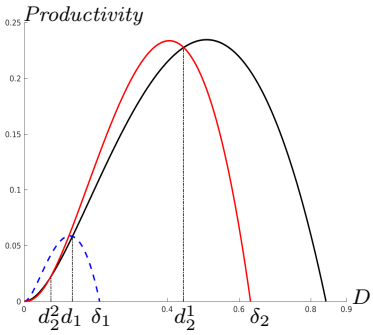

(d) $r = 0.75$, $S^{in} = 2$

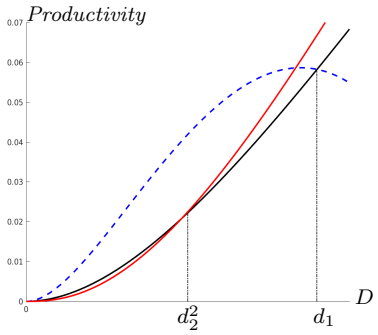

(e) Zoom of (d) showing d_1 and d_2^2

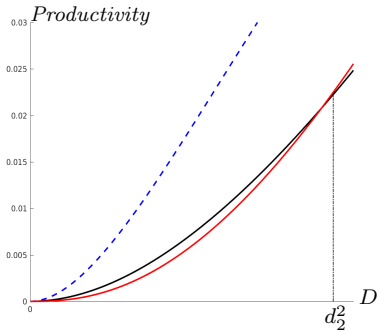

(f) Zoom of (e) showing d_2^2

FIGURE 5. The functions $D \mapsto P_1(S^{in}, D, r)$ (in blue), $D \mapsto P_2(S^{in}, D, r)$ (in red) and $D \mapsto P(S^{in}, D)$ (in black). The bifurcation values d_1, d_2^1, d_2^2, δ_1 and δ_2 are depicted in Figure 4.

functions p_2^1 and p_2^2 are the solutions of equation $f_1(S^{in}) = h_1(S^{in})$. Recall that $h_1(S^{in})$ is given by (33) and $f_1(S^{in}) = f(-\alpha S^{in} + \beta, S^{in})$. We have the limits

$$\lim_{D \to r(m-a)} \beta = +\infty, \qquad \lim_{D \to r(m-a)} \eta = \frac{a^2}{m}, \qquad \lim_{D \to r(m-a)} \rho = +\infty.$$

Therefore, the graph of $y = f_1(S^{in})$ converges toward the horizontal line $y = f(+\infty) = m$, while the graph of $y = h_1(S^{in})$, goes to infinity when $D \to r(m-a)$. Indeed, the curve $y = h_1(S^{in})$ is an hyperbola with fixed vertical asymptote $S^{in} = \lambda(D + a)$ and its horizontal asymptote converges to $y = a^2/m$ and, since $\rho \to \infty$, the hyperbola moves right and converges to infinity. Therefore, $p_1^2(D, r)$ and $p_2^2(D, r)$, the solutions of equation $f_1(S^{in}) = h_1(S^{in})$, converge toward $+\infty$ when $D \to r(m-a)$. □

If the functions $D \mapsto p_2^1(D, r)$ and $D \mapsto p_2^2(D, r)$ are increasing, then they admit inverse functions $S^{in} \mapsto d_2^1(S^{in}, r)$, and $S^{in} \mapsto d_2^2(S^{in}, r)$, respectively, and the equation $S^{in} = p_2^k(D, r)$ is equivalent to the equation $D = d_2^k(S^{in}, r)$, $k = 1, 2$. More precisely, we add the following assumption and notation.

Assumption 4. For every $r \in (0, 1)$, the functions $D \mapsto p_2^k(D, r)$, $k = 1, 2$, are increasing.

Notation 4. Let $S^{in} \mapsto d_2^k(S^{in}, r)$, $k = 1, 2$, be the inverse functions of the functions $D \mapsto p_2^k(D, r)$, $k = 1, 2$, respectively. They are defined for $S^{in} \geq \lambda(a)$.

Theorem 5. *Assume that Assumptions 1, 2 and 4 are satisfied. Then $P_2(S^{in}, D, r) > P(S^{in}, D)$ if and only if $d_2^2(S^{in}, r) < D < \min(\delta_2(S^{in}, r), d_2^1(S^{in}, r))$.*

Proof. Let $r \in (0, 1)$. The functions $D \mapsto p_2^1(D, r)$ and $D \mapsto p_2^2(D, r)$ are increasing. Therefore, the property $d_2^2(S^{in}, r) < D < \min(\delta_2(S^{in}, r), d_2^1(S^{in}, r))$ is satisfied if and only if $\max(\lambda(D/r +$

$a), p_2^1(D,r)) < S^{in} < p_2^2(D,r)$. According to Theorem 3, this is equivalent to $P_2(S^{in},D,r) > P(S^{in},D)$. □

Let us illustrate the results of Theorems 4 and 5 in the particular case corresponding to the Figure 2. This figure is reproduced in Figure 4 with the addition of bifurcation values δ_1 and δ_2, d_1, d_2^1 and d_2^2, defined in Lemma 4, Assumption 3, and Assumption 4, respectively. The graphs of the functions $D \mapsto P(S^{in},D)$, $P_1(S^{in},D,r)$ and $P_2(S^{in},D,r)$, defined by (8), (6) and (7), respectively, and corresponding to the value $S^{in} = 2$ are shown in Figure 5. The productivity of a stable steady state is drawn in bold, while it is drawn in dotted line, when the steady state is unstable. It appears that all inequalities $P_2 > P$, $P_1 > P$ and $P_1 > P_2$ can take place.

In Figure 5, panel (a), and the zoom in panel (b), one sees that for $0 < D < \delta_2$ one has $P_1 > P$ and E_1 is unstable, and for $\delta_2 < D < d_1$ one has $P_1 > P$ and E_1 is stable. One sees also in panel (d), and the zoom in panel (e) that for $0 < D < d_1$ one has $P_1 > P$ and E_1 is unstable. Similarly, the zooms in panels (b) and (c) show that for $d_2^2 < D < \delta_2$ one has $P_2 > P$ and the zooms in panels (e), (f) show that for $d_2^2 < D < d_2^1$ one has $P_2 > P$. Notice that when $P_1 > P_2$ then necessarily E_1 is unstable. On the other hand, the inequality $P_1 > P$ can be satisfied whether E_1 is stable or unstable.

In practice, and as already mentioned at the end of Section 3.1, if the operating parameters are such that $P_1 > P$ or $P_1 > P_2$, to optimize biomass productivity, it is sufficient to take a single tank of volume $V_2 = (1-r)V$, i.e. of a volume less than the total volume V.

This surprising result is due to mortality, since as recalled in Proposition 1 it does not occur when mortality is neglected. Another difference between the case without mortality and the case with mortality is worth noting. In the case without mortality, it is proved that the productivity P_2 never exceed the maximal productivity of the single chemostat. Indeed we have

Proposition 5. [2] *In the case $a = 0$, for any $S^{in} > 0$, $r \in (0,1)$ and $D \in [0, rf(S^{in}))$, we have $P_2(S^{in},D,r) < \overline{P}(S^{in})$, where $\overline{P}(S^{in}) = \max_{0 \le D \le f(S^{in})} P(S^{in},D)$.*

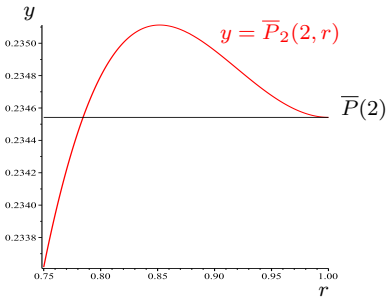

FIGURE 6. The map $r \mapsto \overline{P}_2(S^{in},r)$ with $f(S) = 4S/(5+S)$, $a = 0.3$ and $S^{in} = 2$.

It should be noted that in [2] the result of Proposition 5 was established for the biogas flow rate, see Proposition 6 in [2]. However, in the case of no mortality, the biogas flow rate and the productivity are given by the same expression. Therefore, the result of Proposition 6 of [2] also applies to the productivity.

Remark 4. From Figure 5(d), it is questionable whether the introduction of mortality allows P_2 to take on larger values than the maximum, relative to D, of P. This behaviour does occur as shown in Figure 6.

In Figure 6 we have fixed the biological parameters as in Figure 5 and for $S^{in} = 2$, we have represented the function $r \mapsto \overline{P}_2(S^{in},r)$ defined by

$$\overline{P}_2(S^{in},r) = \max_{0 \le D \le \delta_2(S^{in},r)} P_2(S^{in},D,r).$$

It can be seen that there exists $r^*(S^{in}) \in (0,1)$ such that for any $r \in (r^*(S^{in}),1)$ we have

$$\overline{P}_2(S^{in},r) > \overline{P}(S^{in}).$$

It appears in Figure 6 that $r^*(2) \approx 0.784$. Therefore for the case depicted in Figure 5(d), done with $r = 0.75$, the maximum of P_2 is smaller than the maximum P. However, for $r = 0.85$, for example, the maximum of P_2 will be larger than the maximum P.

When mortality is taken into account in the model, the biogas flow rate and the productivity are no longer given by the same expression. It was shown in [3] that for the biogas flow rate, the behaviour described in Figure 6 always occurs, i.e. there is $r^* \in (0, 1)$ such that for any $r \in (r^*, 1)$, the maximum, relative to D, of $G_2(S^{in}, D, r)$ will be larger than the maximum $G(S^{in}, D)$. Here $G_2(S^{in}, D, r)$ is the biogas flow rate of the serial configuration at steady state E_2 and $G(S^{in}, D)$ is the biogas flow rate of the single chemostat, see [1, 3]. This result was obtained by showing that the first partial derivative in $r = 1$ (at left) of

$$\overline{G}_2(S^{in}, r) = \max_D G_2(S^{in}, D, r)$$

is zero and its second partial derivative is positive, see Proposition 8 in [3]. We were not able to calculate partial derivatives of the productivity, as in the case of biogas, because the calculations are very complicated. We conjecture that such a result on the first and second partial derivatives of $\overline{P}_2(S^{in}, r)$ is also true.

4. The most efficient serial device

In this section we address the following problem: assume that S^{in} and D are fixed. What is the value of r which gives the highest value for the productivity of the serial configuration. As we have seen in Theorems 2 and 3, maximum productivity can be achieved at steady state E_1 or E_2. Therefore we will consider the functions $r \mapsto P_1(S^{in}, D, r)$ and $r \mapsto P_2(S^{in}, D, r)$ and look for the value of r that gives the maximum. The following lemmas describe the domain of definition of the these functions.

Lemma 6. *Let (S^{in}, D) such that $f(S^{in}) > D + a$. Then the function $r \mapsto P_1(S^{in}, D, r)$ is defined for $0 \leq r \leq 1 - r_0(S^{in}, D)$, where $r_0(S^{in}, D) = \frac{D}{f(S^{in})-a}$. Moreover*

$$P_1(S^{in}, D, 0) = P(S^{in}, D), \qquad P_1(S^{in}, D, 1 - r_0(S^{in}, D)) = 0.$$

Proof. The productivity P_1 is defined where the steady state E_1 is also defined. That is to say, P_1 is defined if and only if $S^{in} \geq \lambda\left(\frac{D}{1-r} + a\right)$, which is equivalent to the condition $0 \leq D \leq (1 - r)(f(S^{in}) - a)$. Therefore, if (S^{in}, D) is such that $f(S^{in}) > D + a$, then $P_1(S^{in}, D, r)$ is defined for $r \in \big[0, 1 - r_0(S^{in}, D)\big]$, where $r_0(S^{in}, D)$ is as in the lemma. If $r = 0$, then from the definitions (8) and (6) of P and P_1, respectively, it is seen that $P_1(S^{in}, D, 0) = P(S^{in}, D)$. On the other hand, if $r = 1 - r_0(S^{in}, D)$, then $\overline{x}_2 = 0$, so that $P_1(S^{in}, D, r) = 0$. This case corresponds to a transcritical bifurcation of E_1 and E_0, see Remark 1 in [3]. □

Lemma 7. *Let (S^{in}, D) such that $f(S^{in}) > D + a$. Then the function $r \mapsto P_2(S^{in}, D, r)$ is defined for $r_0(S^{in}, D) \leq r \leq 1$, where r_0 is as in Lemma 6. Moreover, $P_2(S^{in}, D, 1) = P(S^{in}, D)$ and*

$$P_2(S^{in}, D, r_0(S^{in}, D)) = \begin{cases} P_1(S^{in}, D, r_0(S^{in}, D)) & \text{if} \quad r \leq 1/2 \\ 0 & \text{if} \quad r \geq 1/2 \end{cases}$$

Proof. The productivity P_2 is defined where the steady state E_2 is also defined. That is to say, P_2 is defined if and only if $S^{in} \geq \lambda\left(\frac{D}{r} + a\right)$, which is equivalent to the condition $0 \leq D \leq r(f(S^{in}) - a)$. Therefore, if (S^{in}, D) is such that $f(S^{in}) > D + a$, then P_2 is defined for $r \in \big[r_0(S^{in}, D), 1\big]$, where $r_0 = \frac{D}{f(S^{in})-a}$. One has $\lim_{r\to 1} S_2^* = \lambda(D + a)$, see Lemma 3 in [3]. Hence, if $r = 1$, then from $S_1^* = \lambda(D + a)$, and the definitions (8) and (7) of P and P_2, respectively, it is seen that $P_2(S^{in}, D, 1) = P(S^{in}, D)$. On the other hand, if $r = r_0(S^{in}, D)$, then two cases must be distinguished. If $r \geq 1/2$, then $x_2^* = 0$, so that $P_2(S^{in}, D, r) = 0$. If $r \leq 1/2$, then $x_2^* = \overline{x}_2$, so that $P_2(S^{in}, D, r) = P_1(S^{in}, D, r)$. The first case corresponds to a transcritical bifurcation of E_2 and E_0, and the second one to a transcritical bifurcation of E_2 and E_1, see Remark 1 in [3]. □

4.1. **The most efficient serial configurations.** We consider the optimization problems: given a total volume V of two chemostats in series, find the optimal volume distribution that maximize the productivity P_i, $i = 1, 2$, subject to the constraints $V_1 \geq 0$, $V_2 \geq 0$ and $V_1 + V_2 = V$. Using the variable $r = V_1/V \in [0, 1]$ and the domains of definitions of P_1 and P_2 given in Lemmas 6 and 7, these problems are written:

$$\max_{0\leq r\leq 1-r_0(S^{in},D)} P_1(S^{in}, D, r) \quad \text{and} \quad \max_{r_0(S^{in},D)\leq r\leq 1} P_2(S^{in}, D, r).$$

We denote by $r_i^{opt}(S^{in}, D)$, $i = 1, 2$ the sets of most efficient configurations, i.e.,

$$r_1^{opt}(S^{in}, D) = \operatorname*{argmax}_{0\leq r\leq 1-r_0(S^{in},D)} P_1(S^{in}, D, r) \tag{34}$$

$$r_2^{opt}(S^{in}, D) = \operatorname*{argmax}_{r_0(S^{in},D)\leq r\leq 1} P_2(S^{in}, D, r). \tag{35}$$

It is difficult to determine analytically these sets of most efficient configurations. However, when the biological parameters of the model are known and the operating parameters S^{in} and D are fixed, it is easy to plot the graphs of the functions $r \mapsto P_1(S^{in}, D, r)$ and $r \mapsto P_2(S^{in}, D, r)$ and determine the values of r which give the maximum of P_1 and P_2, see Figures 9, 15 and 18.

4.2. **The case without mortality.** The determination of the most efficient serial device is solved in [2] in the case without mortality. For the convenience of the reader and for comparison purposes, the main characteristics are given here. Let g defined by

$$g(D) = \lambda(D + a) + D\lambda'(D + a), \tag{36}$$

It is proved in [2] that if $S^{in} \leq g(D)$ then for any $r \in (0, 1)$, $P_2(S^{in}, D, r) < P(S^{in}, D)$. On the other hand, if $S^{in} > g(D)$ then it is possible to find $r \in (0, 1)$ such that $P_2(S^{in}, D, r) > P(S^{in}, D)$. More precisely, we assume that the function $r \mapsto g_r(D)$, where $g_r(D)$ is defined by (15) is decreasing. Let $r = r_2(S^{in}, D)$ the solution of equation $S^{in} = g_r(D)$. Then $P_2(S^{in}, D, r) > P(S^{in}, D)$ if and only if $r_2(S^{in}, D) < r < 1$. These results, together with the formula (12) of Proposition 1 allow us to describe the most efficient serial device:

Proposition 6. *When $a = 0$ we have $r_1^{opt}(S^{in}, D) = \{0\}$ for all (S^{in}, D) and*

$$r_2^{opt}(S^{in}, D) = \{1\} \text{ if } S^{in} \leq g(D), \qquad r_2^{opt}(S^{in}, D) \subset (r_2(S^{in}, D), 1) \text{ if } S^{in} \leq g(D).$$

The curves Φ_1 and $\Phi_{1/2}$ together with the curve Γ of equation $S^{in} = g(D)$, divide the set of operating parameters (S^{in}, D) in five regions J_k, $k = 0, \ldots, 4$, see Figure 6 in [2]. When (S^{in}, D) satisfies $S^{in} \leq \lambda(D)$, which correspond to $(S^{in}, D) \in J_0$, the only steady state of the series device is E_0, so that there is no productivity for all $r \in (0, 1)$. Apart from this case, there are only four possible cases, as depicted in Figure 8 of [2]. Consequently, it is only in the regions J_2 and J_3, i.e. for (S^{in}, D) located on the right of the curve Γ, that there are values of r for which $P_2(S^{in}, D, r) > P(S^{in}, D)$.

4.3. **The case with mortality.** When the mortality is included in the model, the situation is much more complicated, precisely because mortality allows the inequalities $P_1 > P_2$ and $P_1 > P$. Let us give some results in this direction.

Lemma 8. *Let $D \in [0, m - a)$. The function $r \mapsto p_1(D, r)$ is defined for $r \in \left(0, 1 - \frac{D}{m-a}\right)$ and satisfies*

$$\lim_{r\to 0} p_1(D, r) = \pi_1(D), \qquad \lim_{r\to 1-\frac{D}{m-a}} p_1(D, r) = +\infty,$$

where

$$\pi_1(D) := \lambda(D + a) + \tfrac{D(D+a)}{a}\lambda'(D + a). \tag{37}$$

Proof. The function $r \mapsto p_1(D,r)$ is defined when $(D,r) \in \mathrm{dom}(p_1)$, that is to say for $D \in [0, m-a)$ and $0 < r < 1 - \frac{D}{m-a}$. The first limit is obtained using L'Hôpital's rule. From (17) it is seen that:

$$\lim_{r\to 0} p_1(D,r) = \lambda(D+a) + \tfrac{D+a}{a} \lim_{r\to 0} \tfrac{D}{(1-r)^2} \lambda'\left(\tfrac{D}{1-r} + a\right) = \lambda(D+a) + \tfrac{D(D+a)}{a}\lambda'(D+a).$$

The second limit follows from $\lim_{D\to m} \lambda(D) = +\infty$. □

If the function $r \mapsto p_1(D,r)$ is increasing, then it admits an inverse function $S^{in} \mapsto r_1(S^{in}, D)$, and the equation $S^{in} = p_1(D,r)$ is equivalent to the equation $r = r_1(S^{in}, D)$. More precisely, we add the following assumption which is satisfied by any concave growth function but also by any Hill function, see Section C.

Assumption 5. For every $D \in [0, m-a)$, the function $r \mapsto p_1(D,r)$ is increasing.

Notation 5. Let $S^{in} \mapsto r_1(S^{in}, D)$ be the inverse function of the function $r \mapsto p_1(D,r)$. It is defined for $S^{in} \geq \pi_1(D)$.

Proposition 7. *Assume that Assumptions 1 and 5 are satisfied.*

- *If $S^{in} \leq \pi_1(D)$ then for any $r \in (0,1)$, $P_1(S^{in}, D, r) < P(S^{in}, D)$.*
- *If $S^{in} > \pi_1(D)$ then $P_1(S^{in}, D, r) > P(S^{in}, D)$ if and only if $0 < r < r_1(S^{in}, D)$. In addition, $P_1(S^{in}, D, r) = P(S^{in}, D)$ for $r = 0$ or $r = r_1(S^{in}, D)$.*

Proof. From Assumption 5, the function $r \mapsto p_1(D,r)$ is increasing. Thus, for any $r \in (0,1)$, one has $p_1(D,r) > \pi_1(D)$. If $S^{in} \leq \pi_1(D)$ then one has $S^{in} < p_1(D,r)$. According to Theorem 2 one deduces that $P_1(S^{in}, D, r) < P(S^{in}, D)$, which proves the first item of the proposition.
If $S^{in} > \pi_1(D)$ then $S^{in} > p_1(D,r)$ if and only if $0 < r < r_1(S^{in}, D)$. Thus, according to the Theorem 2 one deduces that $P_1(S^{in}, D, r) > P(S^{in}, D)$ if and only if $0 < r < r_1(S^{in}, D)$. Notice that the equality $P_1(S^{in}, D, r) = P(S^{in}, D)$ for the limiting case $r = 0$ follows from the definitions (8) and (6) of P and P_1, respectively. In addition, if $r = r_1(S^{in}, D)$ then $S^{in} = p_1(D,r)$, which is equivalent to $P_1(S^{in}, D, r) = P(S^{in}, D)$. □

The result of Proposition 7 allows us to describe the most efficient serial device for P_1:

Proposition 8. *We have $r_1^{opt}(S^{in}, D) = \{0\}$ if $S^{in} \leq \pi_1(D)$ and $r_1^{opt}(S^{in}, D) \subset (0, r_1(S^{in}, D))$ if $S^{in} > \pi_1(D)$.*

The novelty compared to the case without mortality (see Proposition 6) is the possibility to have a better biomass productivity P_1 of the serial device than the single chemostat. Now we consider the optimal device for the productivity P_2.

Lemma 9. *Let $D \in [0, m-a)$. The functions $r \mapsto p_2^1(D,r)$ and $r \mapsto p_2^2(D,r)$ are defined for $r \in \left(\frac{D}{m-a}, 1\right)$ and satisfy*

$$\lim_{r\to 1} p_2^1(D,r) = \pi(D), \qquad \lim_{r\to \frac{D}{m-a}} p_2^1(D,r) = +\infty$$

$$\lim_{r\to 1} p_2^2(D,r) = \lim_{r\to \frac{D}{m-a}} p_2^2(D,r) = +\infty,$$

where

$$\pi(D) = \lambda(D+a) + \tfrac{D(D+a)}{D+2a}\lambda'(D+a). \tag{38}$$

Proof. The functions $r \mapsto p_2^1(D,r)$ and $r \mapsto p_2^2(D,r)$ are defined where the steady state E_2 is defined. That is to say, for $D/r + a < m$, which is equivalent to $r > \frac{D}{m-a}$. From Lemma 3, the functions p_2^1 and p_2^2 are the solutions of equation $f_1(S^{in}) = h_1(S^{in})$. Recall that $h_1(S^{in})$ is given by (33) and $f_1(S^{in}) = f(-\alpha S^{in} + \beta, S^{in})$. We have the limits

$$\lim_{r\to 1} \alpha = 0, \quad \lim_{r\to 1} \beta = \lambda(D+a), \quad \lim_{r\to 1} \eta = \tfrac{a^2}{D+a}.$$

Moreover, using L'Hôpital's rule we have

$$\lim_{r\to 1}\rho = D\lim_{r\to 1}\tfrac{\lambda(D/r+a)-\lambda(D+a)}{1-r} = D^2\lambda'(D+a).$$

Therefore, the graph of $y = f_1(S^{in})$ converges toward the horizontal line $y = f(\lambda(D+a)) = D+a$, while the graph of $y = h_1(S^{in})$ converges toward the hyperbola

$$y = \tfrac{a^2}{D+a} + \tfrac{D^2\lambda'(D+a)}{S^{in}-\lambda(D+a)}.$$

Hence, $p_2^2(D,r)$, the largest solution of equation $f_1(S^{in}) = h_1(S^{in})$ converges toward $+\infty$ and $p_2^1(D,r)$, the smallest solution, converges toward the solution of equation

$$D + a = \tfrac{a^2}{D+a} + \tfrac{D^2\lambda'(D+a)}{S^{in}-\lambda(D+a)}.$$

The solution of this equation is $S^{in} = \pi(D)$, where $\pi(D)$ is given by (38). Therefore $p_2^1(D,r)$ converges to $\pi(D)$ when $r \to 1$. On the other hand, using the limits

$$\lim_{r\to \frac{D}{m-a}} \beta = +\infty, \quad \lim_{r\to \frac{D}{m-a}} \eta = \tfrac{a^2}{m}, \quad \lim_{r\to \frac{D}{m-a}} \rho = +\infty,$$

it is seen that the graph of $y = f_1(S^{in})$ converges toward the horizontal line $y = f(+\infty) = m$, while the graph of $y = h_1(S^{in})$, goes to infinity when $r \to \frac{D}{m-a}$. Indeed, the curve

$$y = h_1(S^{in}) = \eta + \tfrac{\rho}{S^{in}-\lambda(D+a)}$$

is an hyperbola with fixed vertical asymptote $S^{in} = \lambda(D + a)$ and its horizontal asymptote converges to $y = a^2/m$. Since $\rho \to \infty$, the hyperbola moves right and converges to infinity. Therefore, $p_2^1(D,r)$ and $p_2^2(D,r)$, the solutions of equation $f_1(S^{in}) = h_1(S^{in})$ converges toward $+\infty$ when $r \to \frac{D}{m-a}$. □

Remark 5. From the definitions (37) and (38) of π_1 and π, respectively, it is seen that $\pi_1(0) = \pi(0) = \lambda(a)$, and, for all $D \in (0, m-a)$, one has $\pi_1(D) > \pi(D) > \lambda(D+a)$.

If the function $r \mapsto p_2^1(D,r)$ is decreasing, then it admits an inverse function $S^{in} \mapsto r_2(S^{in}, D)$, and the equation $S^{in} = p_2^1(D,r)$ is equivalent to the equation $r = r_2(S^{in}, D)$. On the other hand the function $r \mapsto p_2^2(D,r)$ is positive and tends toward infinity when $r \to D/(m-a)$ or $r \to 1$. It admits a minimum value reached for $r = \overline{r}(D)$. If the function $r \mapsto p_2^2(D,r)$ is decreasing on $\left(\frac{D}{m-a}, \overline{r}(D)\right)$, then it admits an inverse function $S^{in} \mapsto r_3(S^{in}, D)$ on this interval. If the function $r \mapsto p_2^2(D,r)$ is increasing on $(\overline{r}(D), 1)$, then it admits also an inverse function $S^{in} \mapsto r_4(S^{in}, D)$ on this interval. Notice that the equation $S^{in} = p_2^2(D,r)$ is then equivalent to the equations $r = r_3(S^{in}, D)$ and $r = r_4(S^{in}, D)$.

More precisely, we add the following assumptions which can be graphically checked whenever the growth function f is specified, see Section C.

Assumption 6. For every $D \in [0, m-a)$, the function $r \mapsto p_2^1(D,r)$ is decreasing.

Notation 6. Let $S^{in} \mapsto r_2(S^{in}, D)$ be the inverse function of the function $r \mapsto p_2^1(D,r)$. It is defined for $S^{in} \geq \pi(D)$.

Assumption 7. For every $D \in [0, m-a)$, the function $r \mapsto p_2^2(D,r)$ is decreasing on $\left(\frac{D}{m-a}, \overline{r}(D)\right)$ and increasing on $(\overline{r}(D), 1)$.

Notation 7. Let $\pi_2(D)$ be the minimum value of the function $r \mapsto p_2^2(D,r)$:

$$\pi_2(D) = p_2^2\left(D, \overline{r}(D)\right). \tag{39}$$

Let $S^{in} \mapsto r_3(S^{in}, D)$ and $S^{in} \mapsto r_4(S^{in}, D)$ be the inverse functions of the function $r \mapsto p_2^2(D,r)$ on the intervals $\left(\frac{D}{m-a}, \overline{r}(D)\right)$ and $(\overline{r}(D), 1)$, respectively. They are defined for $S^{in} \geq \pi_2(D)$.

Remark 6. If Assumptions (6) and (7) are satisfied then, for all $D \in (r(m-a), 1)$, one has $\pi_2(D) > \pi(D)$. Indeed we have $\pi_2(D) = p_2^2\left(D, \overline{r}(D)\right) > p_2^1\left(D, \overline{r}(D)\right) > \pi(D)$.

Proposition 9. *Assume that Assumptions 1, 2, 6 and 7 are satisfied.*

- *If $S^{in} \leq \pi(D)$ then for any $r \in (r_0(S^{in}, D), 1)$, $P_2(S^{in}, D, r) < P(S^{in}, D)$.*
- *If $\pi_2(D) > S^{in} > \pi(D)$ then $P_2(S^{in}, D, r) > P(S^{in}, D)$ if and only if*

$$\max(r_0(S^{in}, D), r_2(S^{in}, D)) < r < 1.$$

In addition, if $r_2(S^{in}, D) > r_0(S^{in}, D)$, then $P_2(S^{in}, D, r) = P(S^{in}, D)$ for $r = 1$ or $r = r_2(S^{in}, D)$.

- *If $S^{in} > \pi_2(D)$ then $P_2(S^{in}, D, r) > P(S^{in}, D)$ if and only if*

$$\max(r_0(S^{in}, D), r_2(S^{in}, D)) < r < r_3(S^{in}, D) \quad \text{or} \quad r_4(S^{in}, D) < r < 1.$$

In addition, if $r_2(S^{in}, D) > r_0(S^{in}, D)$, then $P_2(S^{in}, D, r) = P(S^{in}, D)$ for $r = 1$, or $r = r_k(S^{in}, D)$, $k = 2, 3, 4$.

Proof. From Assumption 6, the function $r \mapsto p_2^1(D, r)$ is decreasing. Thus, for any $r \in (0, 1)$, one has $p_2^1(D, r) > \pi_2(D)$. If $S^{in} \leq \pi_2(D)$ then one has $S^{in} < p_2^1(D, r)$ and according to Theorem 3 one deduces that $P_2(S^{in}, D, r) < P(S^{in}, D)$, which proves the first item of the proposition.
If $\pi_2(D) > S^{in} > \pi(D)$ then $p_2^2(D, r) > S^{in} > p_2^1(D, r)$ if and only if $r_2(S^{in}, D) < r < 1$. Thus, according to the Theorem 3 one deduces that $P_2(S^{in}, D, r) > P(S^{in}, D)$ if and only if $r_2(S^{in}, D) < r < 1$. If $S^{in} > \pi_2(D)$ then $p_2^2(D, r) > S^{in} > p_2^1(D, r)$ if and only if $r_2(S^{in}, D) < r < r_3(S^{in}, D)$ or $r_4(S^{in}, D) < r < 1$. Thus, according to the Theorem 3, one deduces that $P_2(S^{in}, D, r) > P(S^{in}, D)$ if and only if $r > r_0(S^{in}, D)$ and $r_2(S^{in}, D) < r < r_3(S^{in}, D)$ or $r_4(S^{in}, D) < r < 1$. Notice that the equality $P_1(S^{in}, D, r) = P(S^{in}, D)$ for the limiting case $r = 1$ follows from Lemma (7). In addition, if $r_2(S^{in}, D) > r_0(S^{in}, D)$ and $r = r_k(S^{in}, D)$, $k = 2, 3, 4$, then $S^{in} = p_2^1(D, r)$ or $S^{in} = p_2^2(D, r)$, which is equivalent to $P_2(S^{in}, D, r) = P(S^{in}, D)$. □

The result of Proposition 9 allows us to describe the most efficient serial device for P_2:

Proposition 10. *We have $r_2^{opt}(S^{in}, D) = \{1\}$ if $S^{in} \leq \pi(D)$. If $S^{in} > \pi(D)$ we have*

$$r_2^{opt}(S^{in}, D) \subset (\max(r_0(S^{in}, D), r_2(S^{in}, D)), 1)$$

or

$$r_2^{opt}(S^{in}, D) \subset (\max(r_0(S^{in}, D), r_2(S^{in}, D)), r_3(S^{in}, D)) \cup (r_4(S^{in}, D), 1).$$

Combining the results of the Propositions 7 and 9 we see that the curves Φ_1 and $\Phi_{1/2}$ together with the curves Π_1, Π and Π_2 of equations $S^{in} = \pi_1(D)$, $S^{in} = \pi(D)$ and $S^{in} = \pi_2(D)$, defined by (37), (38) and (39), respectively, divide the set of operating parameters (S^{in}, D) in several regions where the functions $r \mapsto P_1(S^{in}, D, r)$ and $r \mapsto P_2(S^{in}, D, r)$ have different behaviors. We will not try to make a general study, as in the case without mortality. However, in the following section, we will describe some typical cases to show the richness of possible behaviors.

Remark 7. The number of regions in the operating plane depends on the relative position of these curves. From Remarks 5 and 6 it is seen that curve Π is located at the right of curve Φ_1 and at the left of curve Π_1, and that curve Π_2 is at the right of curve Π.

5. Application to Monod growth functions

The aim of this section is to give some illustrations of our results for Monod growth functions, and to provide numerical simulations. However, our result are general and apply to a large class of growth functions. We illustrate this in Appendix C for linear and Hill growth functions.

5.1. Sufficient conditions for Assumptions 2, 3 and 5 to be satisfied.

We first give sufficient conditions that will allow us to verify that the assumptions of our general study are satisfied for the considered growth function.

Proposition 11. *For a growth function f satisfying Assumption 1 (i.e. $f' > 0$) we have the following properties:*

- *If f is twice derivable and $f'' \leq 0$ then Assumptions 2, 3 and 5 are satisfied.*

- *If f is twice derivable and, for all $a \geq 0$ and $S > \lambda(a)$, $f''_a(S) > 0$, where*

$$f_a(S) := \tfrac{1}{f(S)-a}, \tag{40}$$

then Assumptions 2 and 5 are satisfied.

Proof. The proof is given in Section D.2. □

With regard to Assumptions 4, 6 and 7, which concern the p_2^1 and p_2^2 functions, we have not been able to find sufficient conditions on the growth function f that imply these assumptions. Indeed, as the p_2^1 and p_2^2 functions are not determined explicitly, but only implicitly as the solutions of the equation $f_1(S^{in}) = h_1(S^{in})$, it is difficult to analyze their partial derivatives with respect to r and D, as we did for the p_1 function. However, once the growth function f is specified, it is easy to check graphically that Assumptions 4, 6 and 7 are satisfied.

5.2. **Monod Growth function.** We consider the Monod growth function

$$f(S) = \tfrac{mS}{K+S} \tag{41}$$

Note that $m = \sup_{S>0} f(S)$. Since $f'(S) = mK/(K+S)^2 > 0$ and $f''(S) = -2mK(K+S)^2 < 0$, then using the Proposition 11, it is seen that Assumptions 1, 2, 3 and 5 are satisfied. The Assumptions 4, 6 and 7 will be checked graphically. Let us first determine the possible intersection points of curves Π_{r1} and Φ_r, as shown in Figure 7.

Proposition 12. *Curves Π_{r1} and Φ_r intersect at $(\lambda(a), 0)$, and at most at two points $Q_1 = (p_1(d_1, r), d_1)$ and $Q_2 = (p_1(d_2, r), d_2)$ where $d_2 < d_1$ are defined by*

$$d_1 = \tfrac{r(m-2a)+\sqrt{\Delta}}{2}, \quad d_2 = \tfrac{r(m-2a)-\sqrt{\Delta}}{2},$$

with $\Delta = r^2(m-2a)^2 - 4a(m-a)(r^2-3r+1)$. More precisely, let $r_* = \frac{2a(m-a)}{\sqrt{\Delta_1}+3a(m-a)}$, where $\Delta_1 = a(m-a)(m^2+a(m-a)) > 0$. Then $r_* < \frac{3-\sqrt{5}}{2}$ is satisfied for all $a \in (0, m)$ and equality occurs when $a = m/2$. Apart from point $(\lambda(a), 0)$, the intersection points of curves Π_{r1} and Φ_r are given as follows:

- *Assume that $0 < a < m/2$. If $0 < r < r_*$, then curves Π_{r1} and Φ_r do not intersect; if $r = r_*$, then curves Π_{r1} and Φ_r intersect at point $Q_1 = Q_2$; if $r_* < r < \frac{3-\sqrt{5}}{2}$, then curves Π_{r1} and Φ_r intersect at two points $Q_1 \neq Q_2$; if $\frac{3-\sqrt{5}}{2} \leq r < \frac{1}{2}$, then curves Π_{r1} and Φ_r intersect at point Q_1.*
- *Assume that $m/2 \leq a < m$. If $0 < r \leq \frac{3-\sqrt{5}}{2}$, then curves Π_{r1} and Φ_r do not intersect; if $\frac{3-\sqrt{5}}{2} < r < \frac{1}{2}$, then curves Π_{r1} and Φ_r intersect at point Q_1.*

Proof. The proof is given in Appendix D.3 □

Let us illustrate these results for the biological values of the parameters $m = 4$, $K = 5$ and $a = 0.3$ that have been used in Figure 2. For these parameter values we have $a < m/2$ and $r_* = 0.289$. Therefore for $r < 0.289$ or $r \geq 1/2$ curves Π_{r1} and Φ_r have no other point of intersection than the point $(\lambda(a), 0)$. This has been illustrated with $r = 0.25$ and $r = 0.75$ in Figure 2. For $0.289 < r < \frac{3-\sqrt{5}}{2}$, curves Π_{r1} and Φ_r have two points of intersection Q_1 and Q_2, as illustrated in the case $r = 0.3$ in Figure 7(a,b,c). For $r = 0.3$ we have $Q_1 = (10.87, 0.732)$ and $Q_2 = (2.3, 0.29)$. For $\frac{3-\sqrt{5}}{2} \leq r < 1/2$, curves Π_{r1} and Φ_r have only one point of intersection Q_1, as illustrated in the case $r = 0.39$ in Figure 7(d,e,f). For $r = 0.39$ we have $Q_1 = (71.33, 1.34)$. Note that when $r = r_*$ we have $Q_1 = Q_2$, when $r = \frac{3-\sqrt{5}}{2}$ the point Q_2 merges with the point $(\lambda(a), 0)$ and when r tends to $1/2$ the point Q_1 tends to infinity.

The functions p_2^1 and p_2^2 which are defined implicitly as solutions of the equation $f_1 = h_1$, can be given explicitly, as shown in the following proposition.

Proposition 13. *The functions p_2^1 and p_2^2 can be given by explicit formulas.*

Proof. The proof is given in Appendix D.4. □

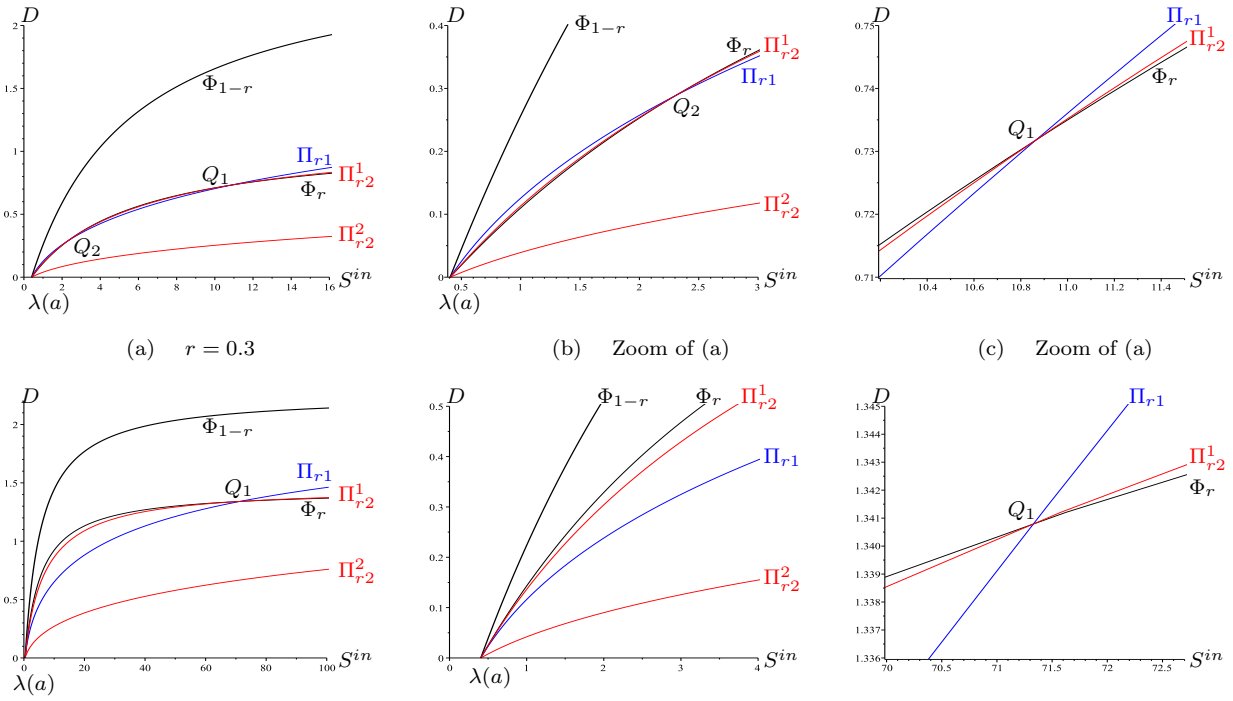

(a) $r = 0.3$ (b) Zoom of (a) (c) Zoom of (a)

(d) $r = 0.39$ (e) Zoom of (d) (f) Zoom of (d)

FIGURE 7. The operating diagram for $f(S) = 4S/(5 + S)$ and $a = 0.3$ showing curves Φ_r and Φ_{1-r} (in black), Π_{r1} (in blue), Π^1_{r2} and Π^2_{r2} (in red) and the intersection points of Φ_r, Π_{r1} and Π^1_{r2}.

TABLE 2. f Monod

$f(S)$	$=$	$\frac{mS}{K+S}$
$\lambda(D)$	$=$	$\frac{KD}{m-D}$
$p_1(D,r)$	$=$	$K\frac{m-a}{a}\frac{(D+a)(D+a-ar)}{(m-D-a)(m-D-a-(m-a)r)}$
$\pi_1(D)$	$=$	$K\frac{m-a}{a}\left(\frac{D+a}{m-D-a}\right)^2$
$\pi(D)$	$=$	$K\frac{2(m-a)-D}{D+2a}\left(\frac{D+a}{m-D-a}\right)^2$
$r_0(S^{in},D)$	$=$	$\frac{D(K+S^{in})}{mS^{in}-a(K+S^{in})}$
$r_1(S^{in},D)$	$=$	$\frac{K(m-a)(D+a)^2-a(m-D-a)^2S^{in}}{a(m-a)(K(D+a)-(m-D-a)S^{in})}$

Proposition 14. *The curve $\Phi_{1/2}$ lies to the right of Π. The curves $\Phi_{1/2}$ and Π_1 intersect at point $Q = (S^{in}_Q, D_Q)$ where*

$$D_Q = \tfrac{m-2a}{2}, \qquad S^{in}_Q = \lambda(m-a).$$

Moreover $\Phi_{1/2}$ lies to the left of Π_1 for $0 < D < D_Q$ and to the right of Π_1 for $D > D_Q$.

Proof. The function $\phi(D) := \pi(D) - \lambda(2D + a)$ is given by

$$\phi(D) = \tfrac{KDm(D^2+a(m-a))}{(D+2a)(m-D-a)^2(m-2D-a)}.$$

One has $\phi(D) > 0$ for all $D \in \left(0, \frac{m-a}{2}\right)$. Therefore $\Phi_{1/2}$ lies to the right of Π.
The function $\phi_1(D) := \lambda(2D + a) - \pi_1(D)$ is given by

$$\phi_1(D) = \tfrac{KmD^2(m-2D-2a)}{a(m-D-a)^2(m-2D-a)}.$$

One has $\phi_1(D_Q) = 0$, $\phi_1(D) > 0$ for $D \in (0, D_Q)$ and $\phi_1(D) < 0$ for $D \in \left(D_Q, \frac{m-a}{2}\right)$. Therefore $\Phi_{1/2}$ and Π_1 intersect at point $Q = (S_Q^{in}, D_Q)$ and $S_Q^{in} = \lambda(2D_Q + a) = \lambda(m - a)$. Their relative position is as in the lemma. □

Remark 8. The result of Proposition 14 complements the one given in Remark 7. The relative position of curve Π_2 (which is only known to be to the right of curve Π) in relation to the other curves, gives a complete description of all possible cases. Once the biological parameters are fixed, the curve Π_2 can be determined numerically and plotted in the operating diagram with the other curves Φ_1, $\Phi_{1/2}$, Π_1 and Π.

We assume that $f(S) = 4S/(5+S)$ and $a = 0.3$, as in Figure 7, and the curve Π_2 is represented numerically, see Figure 8 (a) and (b). It can be seen that curve Π_2 lies to the right of curve Π_1 and $\Phi_{1/2}$. Therefore the six curves Φ_1, $\Phi_{1/2}$, Π_1, Π and Π_2 divide the operating plane in seven regions labeled $\mathcal{J}_k$, $k = 0..6$. Let us illustrate the behavior of the productivities $P_1(S^{in}, D, r)$ and $P_2(S^{in}, D, r)$, as a function of r, for the operating points $o_k \in \mathcal{J}_k$, $k = 1..6$, shown in Figure 8 (a) and (b). We do not consider a point in $\mathcal{J}_0$ since, for such a point, the chemostat and the serial device are washed out.

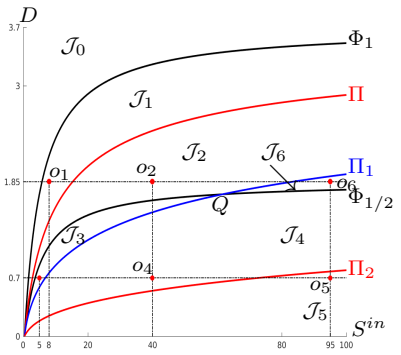

(a)

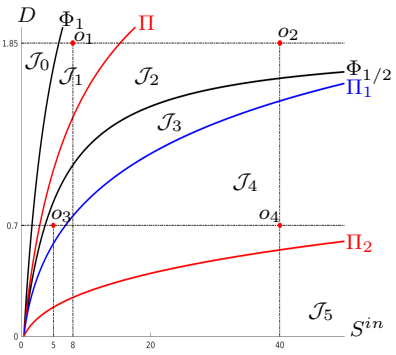

(b): Zoom of (a)

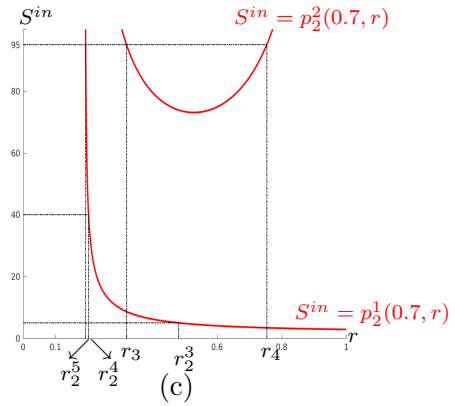

(c)

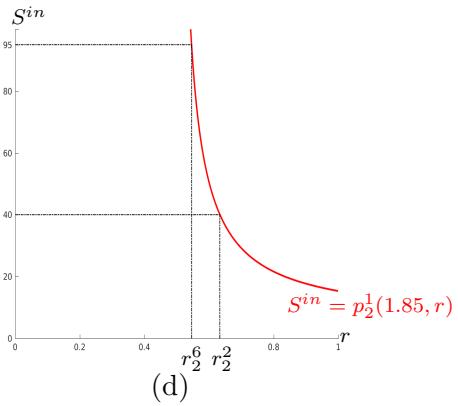

(d)

FIGURE 8. (a) and (b): The curves Φ_1, $\Phi_{1/2}$ (in black), Π_1 (in blue), Π and Π_2 (in red) divide the operating plane in seven regions, $\mathcal{J}_k$, $k = 0..6$ and the operating points $o_k \in \mathcal{J}_k$, $k = 1..6$. (c): The graphical depiction of Assumptions 6 and 7, for $D = 0.7$, showing the values $r_2^k = r_2(S^{in}, D)$, corresponding to o_k, $k = 3..5$, respectively, and the values of r_3 and r_4 corresponding to o_5. (d): The graphical depiction of Assumptions 6, for $D = 1.85$, showing the values $r_2^k = r_2(S^{in}, D)$, corresponding to o_k, $k = 2, 6$, respectively. The operating points are $o_1 = (8, 1.85)$, $o_2 = (40, 1.85)$, $o_3 = (5, 0.7)$, $o_4 = (40, 0.7)$, $o_5 = (95, 0.7)$. and $o_6 = (95, 1.85)$.

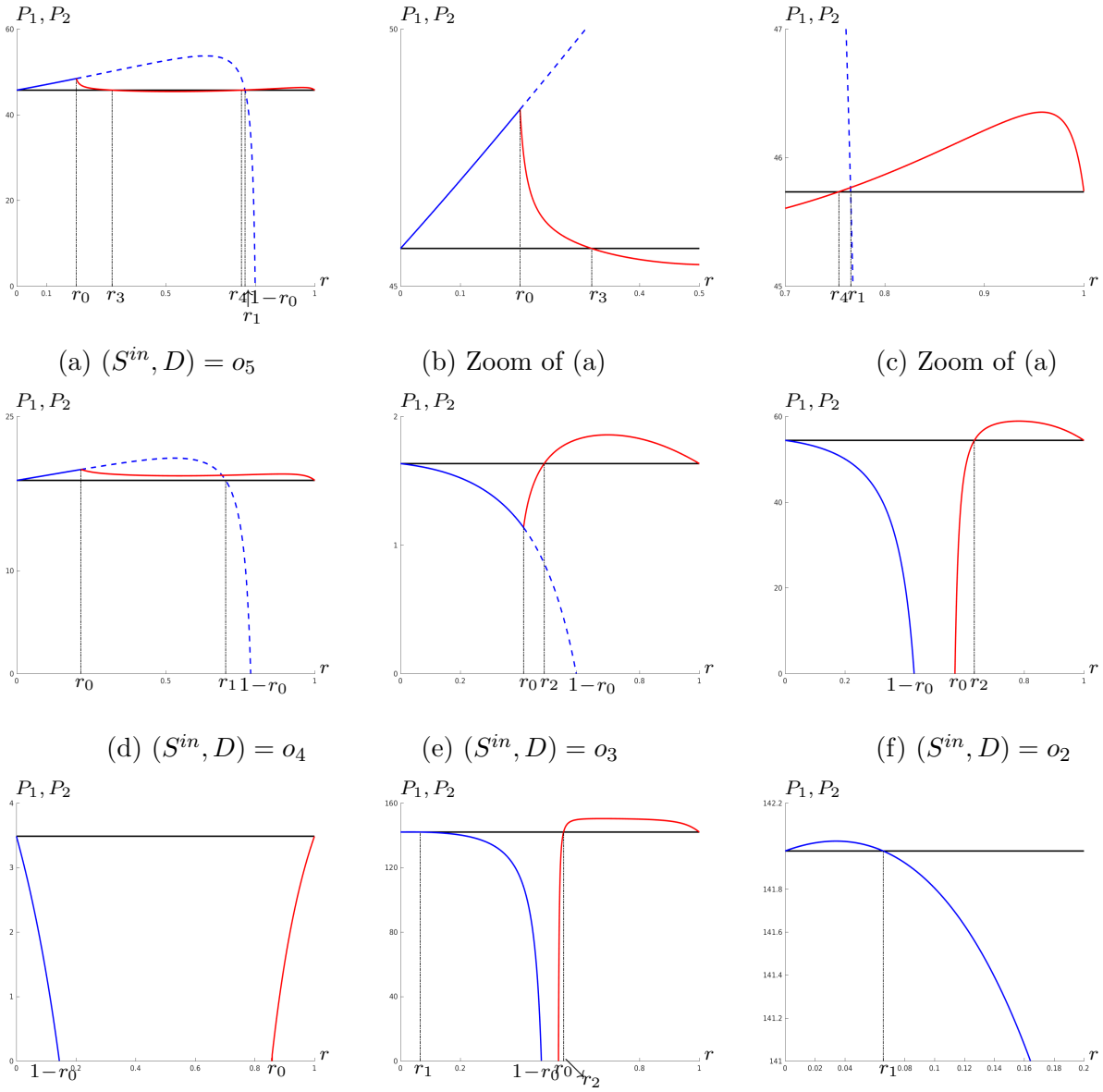

(a) $(S^{in}, D) = o_5$ (b) Zoom of (a) (c) Zoom of (a)

(d) $(S^{in}, D) = o_4$ (e) $(S^{in}, D) = o_3$ (f) $(S^{in}, D) = o_2$

(g) $(S^{in}, D) = o_1$ (h) $(S^{in}, D) = o_6$ (i) Zoom of (h)

FIGURE 9. The curves of the functions $r \mapsto P_2(S^{in}, D, r)$ (in red) and $r \mapsto P_1(S^{in}, D, r)$ (in blue), for S^{in} and D fixed and the corresponding value of $P(S^{in}, D)$ (in black). The r_k values are given in Table 3.

TABLE 3. The values of r_k, corresponding to the operating points $o_1, \dots o_6$ in Figure 8.

	r_0	r_1	r_2	r_3	r_4
$o_6 = (95, 1.85)$	0.529	$0.657\,10^{-1}$	0.546		
$o_5 = (95, 0.7)$	0.2	0.766	0.193	0.32	0.754
$o_4 = (40, 0.7)$	0.215	0.701	0.202		
$o_3 = (5, 0.7)$	0.412		0.481		
$o_2 = (40, 1.85)$	0.568		0.633		
$o_1 = (8, 1.85)$	0.856				

Figure 8 (c) shows the functions $r \mapsto p_2^1(D, r)$ and $r \mapsto p_2^2(D, r)$, for $D = 0.7$ corresponding to the horizontal line $D = 0.7$ depicted in panels (a) and (b) of the figure. It appears that

$r \mapsto p_2^1(D,r)$ is decreasing and $r \mapsto p_2^2(D,r)$ is decreasing and then increasing. Therefore the Assumptions 6 and 7 are satisfied for $f(S) = 4S/(5+S)$, $a = 0.3$ and $D = 0.7$. Figure 8 (c) shows the values of $r_2(S^{in}, D)$ corresponding to the three operating points o_k, $k = 3, 4, 5$ depicted in panels (a) and (b). The figure shows also the values of $r_3(S^{in}, D)$ and $r_4(S^{in}, D)$ corresponding to $o_5 = (4, 0.7)$. The numerical values of r_2, r_3 and r_4, with three digits are collected in Table 3. This table gives also $r_0(S^{in}, D)$ and $r_1(S^{in}, D)$, whose expressions are known analytically, see Table 2.

Figure 8 (d) shows the function $r \mapsto p_2^1(D,r)$ for $D = 1.85$ corresponding to the horizontal line $D = 1.85$ depicted in panels (a) and (b) of the figure. It appears that $r \mapsto p_2^1(D,r)$ is decreasing. Therefore the Assumption 6 is satisfied for $f(S) = 4S/(5+S)$, $a = 0.3$ and $D = 1.85$. Figure 14(d) shows the values of $r_2(S^{in}, D)$ corresponding to the two operating points o_k, $k = 2, 6$ depicted in panels (a) and (b). The numerical values of r_2, with three digits are collected in Table 3.

Figure 9 shows $P_1(S^{in}, D, r)$ and $P_2(S^{in}, D, r)$, as functions of r, for the six operating points o_k, $k = 1..6$ shown in Figure 8 (a) and (b). Let us first recall the theoretical predictions.

Since $o_6 = (95, 1.85) \in \mathcal{J}_6$, this operating point satisfies the condition $\pi_2(D) > \lambda(2D + a) > S^{in} > \pi_1(D) > \pi(D)$. Hence, from Proposition 7 it is deduced that $P_1(95, 1.85, r) > P(95, 1.85)$ if and only if $0 < r < r_1$. Moreover, from Proposition 9 it is deduced that $P_2(95, 1.85, r) > P(95, 1.85)$ if and only if $r_2 = \max(r_0, r_2) < r < 1$. This behavior is illustrated in Figure 9 (h), showing the values r_1, $1 - r_0$, r_0 and r_2 and the zoom in panel (i) showing the value r_1.

Since $o_5 = (95, 0.7) \in \mathcal{J}_5$, this operating point satisfies the condition $S^{in} > \pi_2(D) > \pi_1(D)$. Hence, from Proposition 7 it is deduced that $P_1(95, 0.7, r) > P(95, 0.7)$ if and only if $0 < r < r_1$. Moreover, from Proposition 9 it is deduced that $P_2(95, 0.7, r) > P(95, 0.7)$ if and only if $r_0 = \max(r_0, r_2) < r < r_3$ or $r_4 < r < 1$. This behavior is illustrated in Figure 9 (a), the zoom in panel (b) showing the values r_0 and r_3, and the zoom in panel (c), showing the values r_4 and r_1.

On the other hand, since $o_4 = (40, 0.7) \in \mathcal{J}_4$, this operating point satisfies the condition $\pi_2(D) > S^{in} > \pi_1(D) > \pi(D)$. Hence, from Proposition 7 it is deduced that $P_1(40, 0.7, r) > P(40, 0.7)$ if and only if $0 < r < r_1$, and, from Proposition 9 it is deduced that $P_2(40, 0.7, r) > P(40, 0.7)$ if and only if $r_0 = \max(r_0, r_2) < r < 1$. This behavior is illustrated in Figure 9(d).

Since $o_3 = (5, 0.7) \in \mathcal{J}_3$, this operating point satisfies the condition $\pi_1(D) > S^{in} > \lambda(2D + a) > \pi(D)$. Hence, from Proposition 7 it is deduced that $P_1(5, 0.7, r) < P(5, 0.7)$ for any $r \in (0, 1 - r_0)$. Moreover, from Proposition 9 it is deduced that $P_2(5, 0.7, r) > P(5, 0.7)$ if and only if $r_2 = \max(r_0, r_2) < r < 1$. This behavior is illustrated in Figure 9(e), showing the values r_0, r_2 and $1 - r_0$.

Since $o_2 = (40, 1.85) \in \mathcal{J}_2$, this operating point satisfies the condition $\pi_1(D) > \lambda(2D + a) > S^{in} > \pi(D)$. Hence, from Proposition 7 it is deduced that $P_1(40, 1.85, r) < P(40, 1.85)$ for any $r \in (0, 1 - r_0)$. Moreover, from Proposition 9 it is deduced that $P_2(40, 1.85, r) > P(40, 1.85)$ if and only if $r_2 = \max(r_0, r_2) < r < 1$. This behavior is illustrated in Figure 9 (f), showing the values $1 - r_0$, r_0 and r_2.

Finally, since $o_1 = (8, 1.85) \in \mathcal{J}_1$, this operating point satisfies the condition $\pi_1(D) > \lambda(2D + a) > S^{in} > \pi(D)$. Hence, from Proposition 7 it is deduced that $P_1(8, 1.85, r) < P(8, 1.85)$ for any $r \in (0, 1 - r_0)$. Moreover, from Proposition 9 it is deduced that $P_2(8, 1.85, r) < P(8, 1.85)$ for any $r_0 < r < 1$. This behavior is illustrated in Figure 9 (g), showing the values $1 - r_0$ and r_0.

Recall that when $r_0 < 1/2$, then r_0 corresponds to a transcritical bifurcation of E_2 and E_1, while when $r_0 > 1/2$, then r_0 corresponds to a transcritical bifurcation of E_2 and E_0. The first case can be seen in Figure 9 (a), (b), (d) and (e), and the second case can be seen in Figure 9 (g), (h) and (i). Recall also that $1 - r_0$ corresponds to a transcritical bifurcation of E_1 and E_0, which is observed in 9 (a), (d), (e), (f), (g) and (h).

Figure 9 shows that for the operating points o_5 and o_4 the most efficient device is obtained for $r_1^{opt}(o_5) \approx 0.635$ and $r_1^{opt}(o_4) \approx 0.528$. For these operating points, the productivity P_1 of the unstable steady state E_1 for $r = r_1^{opt}$ is significantly higher than the productivity P of the single chemostat and the productivity P_2 of the positive steady state E_2. On the other hand, for the operating points o_3, o_2 and o_6, the most efficient device is obtained for $r_2^{opt}(o_3) \approx 0.694$,

$r_2^{opt}(o_2) \approx 0.782$ and $r_2^{opt}(o_6) \approx 0.676$. For these operating points, the productivity of the serial device is obtained with the coexistence steady state E_2.

6. Conclusion

The aim of this article was to generalize, to the case of mortality, the results obtained in [2] on the productivity of two interconnected chemostats in series. The main question we have looked at is:

Question 1. What are the three operating conditions, i.e. the distribution of the total volume between the two chemostats, the dilution rate and the input substrate concentration, for which the productivity of the serial configuration is larger than the productivity of the single chemostat ?

A first caveat is in order: the productivity of the biomass at the steady state where the species is maintained in both chemostats is not always larger than the productivity of the biomass at the steady state where the species in maintained only in the second chemostat, as it was the case when there is no mortality in the model. Therefore, in Question 1 we need to specify in which steady state the system is. We have answered this question for the both steady states (see Theorems 2 and 3). In particular, the productivity at the steady state where the species is maintained only in the second chemostat can be larger than the productivity of the single chemostat. In the case of no mortality this never happens. The answer to this question allowed us to consider and fully answer the following questions:

Question 2. Assuming that two operating parameters which are the distribution of the total volume between the two chemostats and the input substrate concentration are fixed, what are the values of the third operating parameter, i.e. the dilution rate, for which the productivities (at both steady states) of the serial coexistence is larger than the productivity of the single chemostat ?

Question 3. Assuming that two operating parameters which are the input substrate concentration and the dilution rate are fixed, what are the values of the third operating parameter, i.e. the distribution of the total volume between the two chemostats, for which the productivities (at both steady states) of the serial coexistence is larger than the productivity of the single chemostat ?

These questions are of biological importance since the answers give which type of bioreactor (single or in series) is best suited for the productivity. Indeed, the conditions under which the serial configuration is either beneficial or detrimental to the productivity of both steady states are completely described.

We have answered Question 2 in Section 3.3 where we analyzed the behaviour of the productivity with respect of the dilution rate. We have answered Question 3 in Section 4 where we analyzed the behavior of the productivity with respect of the distribution of the total volume between the two chemostats.

Figures 9, 15 and 18 show that the answers to Questions 1, 2 and 3 are more subtle than in the case without mortality. In particular, the productivity of the steady state where the species is maintained in both chemostats can be larger than the productivity of the single chemostat for configurations where the volume of the first reactor is either sufficiently small or sufficiently large (close to the total volume). In the case of no mortality, this only occurs when the volume of the first reactor is large enough.

What is also new compared to the case without mortality is that for a fixed input substrate concentration, if the practitioner can choose the dilution rate then the series configuration becomes the structure that should be considered. This property is due to mortality, because in the case without mortality, it was shown in [2] that the productivity of the serial device is always smaller than the maximum, relative to the dilution rate, of the productivity of the single chemostat. When there is a mortality in the model, then Figure 6 gives numerical evidence that the serial configuration can have a larger productivity than the maximum, with respect of the

dilution rate, of the productivity of the single chemostat. This property was also shown for the biogas flow rate in [3]. However it is an open question if the property is always true for the productivity. We think this problem is difficult and warrants further work.

Acknowledgements

The authors thank Alain Rapaport and Jérôme Harmand for valuable and fruitful discussions about this work. The authors thank the Euro-Mediterranean research network Treasure (`http://www.inra.fr/treasure`) for support.

Appendix A. The single chemostat

The mathematical equations representing the single chemostat are given by (3), where S and x denote respectively the substrate and the biomass concentration, S^{in} the input substrate concentration, a the mortality rate and D the dilution rate. It is well known (see [6]) that, besides the washout $F_0 = (S^{in}, 0)$, that this system can have a positive steady state $F_1 = (S^*(D), x^*(S^{in}, D)$, where

$$S^* = \lambda(D + a) \quad \text{and} \quad x^* = \tfrac{D}{D+a}(S^{in} - \lambda(D + a)).$$

See Figure 10(a) for the plot of the functions $D \mapsto S^*(D)$ and $D \mapsto x^*(S^{in}, D)$ for $0 \le D \le \delta$, where $\delta = f(S^{in}) - a$. The conditions of existence and stability of the steady states are given in Table 4. Therefore, the curve Φ defined by

$$\Phi := \{(S^{in}, D) : D = f(S^{in}) - a\} = \{(S^{in}, D) : S^{in} = \lambda(D + a)\}. \tag{42}$$

splits the set of operating parameters (S^{in}, D) into two regions denoted I_0 and I_1 defined in Table 4 and depicted in Figure 10(c). The asymptotic behaviour of the system in these regions is as depicted in Table 4.

Table 4. The conditions of existence and stability of the steady states of (3) and the asymptotic behavior in the regions I_0 and I_1 of the operating diagram.

	Existence condition	Stability condition
F_0	Always exists	$D > f(S^{in}) - a$
F_1	$D < f(S^{in}) - a$	Stable if it exists

	F_0	F_1
$I_0 := \{(S^{in}, D) : D \ge f(S^{in}) - a\}$	GAS	
$I_1 := \{(S^{in}, D) : D < f(S^{in}) - a\}$	U	GAS

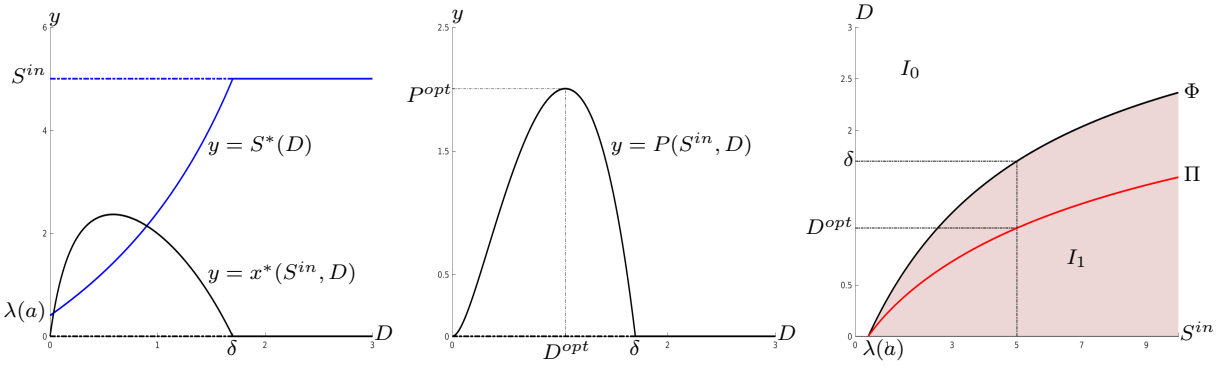

(a) (b) (c)

Figure 10. (a): The functions $D \mapsto S^*(D)$ (in blue) and $D \mapsto x^*(S^{in}, D)$ (in black). (b): The function $D \mapsto P(S^{in}, D)$ with $D^{opt} = D^{opt}(S^{in})$ and $P^{opt} = P(S^{in}, D^{opt}(S^{in}))$. (c): The operating diagram and the curve Π. The figure is done with $f(S) = 4S/(5 + S)$, $a = 0.3$ and $S^{in} = 5$ in panels (a) and (b).

The productivity of (3) at steady state F_1 is given by (8), that we recall here

$$P(S^{in}, D) := Qx^* = \frac{VD^2}{D+a}(S^{in} - \lambda(D+a)). \tag{43}$$

For S^{in} fixed, the function $D \mapsto P(S^{in}, D)$ is defined for $0 \leq D \leq \delta := f(S^{in}) - a$. It is positive for $0 < D < f(S^{in}) - a$ and equal to 0 for $D = 0$ and $D = \delta$, see Figure 10(b). Therefore it attains a maximum for some value

$$D^{opt}(S^{in}) := \underset{0 \leq D \leq f(S^{in})-a}{\operatorname{argmax}} P(S^{in}, D). \tag{44}$$

which is assumed to be unique.

Proposition 15. *The dilution rate $D^{opt}(S^{in})$ defined by (44) is the solution of equation $S^{in} = \pi(D)$ where π is defined by (38).*

Proof. For all $D < f(S^{in}) - a$ we have

$$\frac{\partial P}{\partial D}(S^{in}, D) = \frac{VD(D+2a)}{(D+a)^2}\left(S^{in} - \lambda(D+a)\right) - \frac{VD^2}{D+a}\lambda'(D+a) = \frac{VD(D+2a)}{(D+a)^2}(S^{in} - \pi(D)).$$

with π defined by (38). Therefore, $\frac{\partial P}{\partial D}(S^{in}, D) = 0$ is verified if and only if $S^{in} = \pi(D)$. □

Therefore, the curve Π defined by equation $S^{in} = \pi(D)$ is the set of operating parameters for which the productivity is maximal, see Figure 10(c).

We recall that the biogas flow rate of the single chemostat is defined by (see [1, 2, 3, 12, 14])

$$G(S^{in}, D) := Vx^* f(S^*) = VD(S^{in} - \lambda(D+a)).$$

For the single chemostat, without mortality rate of the biomass, the biogas flow rate $G(S^{in}, D)$ and the productivity of the biomass are given by the same function of the operating parameters:

$$P(S^{in}, D) = VD(S^{in} - \lambda(D)) = G(S^{in}, D).$$

However, this is no longer the case when mortality is taken in consideration. For the study of the biogas flow rate of the serial configuration, the reader can consult [3].

Appendix B. Some useful results on the serial configuration

B.1. **Graphical interpretation of S_2^*.** Let S^{in} be fixed such that $f(S^{in}) < D_1 + a$. Figure 11(a) shows the graphs of functions $S_2 \mapsto f(S_2)$ and $S_2 \mapsto h(S_2, S^{in})$, and the solution S_2^* of the equation $f(S_2) = h(S_2, S^{in})$, which is unique since f is increasing and the graph of the function $S_2 \mapsto h(S_2, S^{in})$ is a decreasing hyperbola. This proves the uniqueness, if it exists, of the steady state E_2.

Actually, the function h depends on all operating parameters S^{in}, D_1 and D_2. However, to avoid unnecessary cumbersome notations, we have highlighted the dependence of h only on the operating parameter S^{in}, because of its crucial importance for the property to be discussed, namely that S_2^* decreases as S^{in} increases, see Figure 11(b).

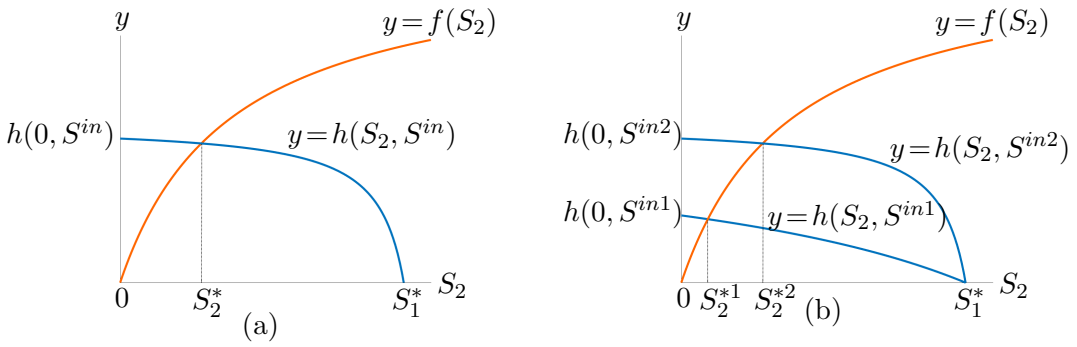

Figure 11. (a): Graphical illustration of equation $h(S_2, S^{in}) = f(S_2)$, showing the uniqueness of the solution S_2^*. (b): The function $S^{in} \mapsto S_2^*(S^{in})$ is decreasing.

Remark 9. This result means that the effluent steady state concentration of substrate decreases when the influent concentration of substrate increases. This behavior is very different from the classical one bioreactor case, where the effluent steady state substrate concentration is independent of the influent substrate concentration.

From Figure 11 it is seen that $S_2^* < S_1^* = \lambda\left(\frac{D}{r} + a\right)$. If $a = 0$ we also have $S_2^* < \lambda\left(\frac{D}{1-r}\right)$ as stated in the following lemma.

Lemma 10. *Assume that $a = 0$. For all $r \in (0,1)$, S^{in} and D such that $D < rf(S^{in})$ we have $S_2^* < \lambda(D/(1-r))$.*

Proof. Assume that $a = 0$ and $D < rf(S^{in})$, i.e. $\lambda(D/r) < S^{in}$. Recall that S_2^* is the unique solution of $f(S_2) = h(S_2, S^{in})$ where, in the case $a = 0$, h_2 defined by (27) becomes :

$$h(S_2, S^{in}) = \frac{D}{1-r}\frac{S_1^* - S_2}{S^{in} - S_2}, \qquad \text{where} \qquad S_1^* = \lambda\left(\frac{D}{r}\right).$$

If $\lambda\left(\frac{D}{1-r}\right) \geq S^{in}$ then one has $S_2^* < \lambda\left(\frac{D}{r}\right) < S^{in} \leq \lambda\left(\frac{D}{1-r}\right)$. Assume that $\lambda\left(\frac{D}{1-r}\right) < S^{in}$. We have

$$\frac{S_1^* - \lambda\left(\frac{D}{1-r}\right)}{S^{in} - \lambda\left(\frac{D}{1-r}\right)} < 1 \Longrightarrow h\left(\lambda\left(\frac{D}{1-r}\right)\right) < \frac{D}{1-r} = f\left(\lambda\left(\frac{D}{1-r}\right)\right) \Longrightarrow S_2^* < \lambda\left(\frac{D}{1-r}\right)$$

The last implication follows from the fact that f is increasing and h_2 is decreasing. □

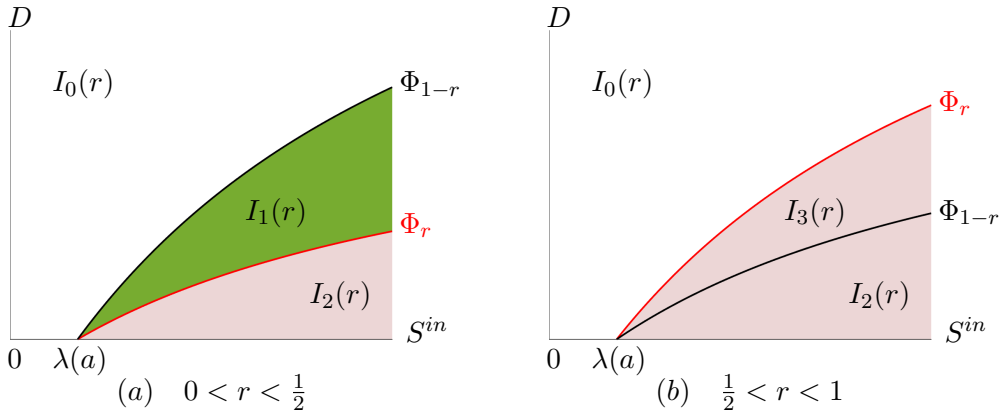

FIGURE 12. The operating diagram of (2): (a) the region $I_3(r)$ is empty; (b) the region $I_1(r)$ is empty.

B.2. **Operating diagram.** We fix $r \in (0,1)$ and we depict in the plane (S^{in}, D) the regions in which the solution of system (2) globally converges towards one of the steady states E_0, E_1 or E_2. Let Φ_r be the curve defined by

$$\Phi_r = \left\{(S^{in}, D) \in \mathbb{R}_+^2 : D = r(f(S^{in}) - a)\right\} = \left\{(S^{in}, D) \in \mathbb{R}_+^2 : S^{in} = \lambda\left(\frac{D}{r} + a\right)\right\} \tag{45}$$

Proposition 16. [3] *The curves Φ_r and Φ_{1-r}, defined by (45) separate the operating plane (S^{in}, D), in the regions $I_k(r)$, $k = 0, 1, 2, 3$, see Figure 12, and defined in the Table 5. The behavior of the system, when the region is not empty, is given in Table 5*

In Table 5, U means that the steady state is unstable, GAS means that the steady state is globally asymptotically stable in the positive orthant and no letter means that the steady state does not exist.

APPENDIX C. APPLICATIONS TO LINEAR AND HILL GROWTH FUNCTIONS

C.1. **Linear growth functions.** In this section we apply our results to the linear growth function $f(S) = \gamma S$, with $\gamma > 0$. Note that $m = \sup_{S>0} f(S) = +\infty$. Since $f' = \gamma$ and $f'' = 0$, then using the Proposition 11, it is seen that Assumptions 1, 2, 3 and 5 are satisfied. The Assumptions 4, 6 and 7 will be checked graphically. Let us first determine the possible intersection points of curves Π_{r1} and Φ_r, as shown in Figure 13.

TABLE 5. Stability of the steady states in the various regions of the operating diagram.

Region	E_0	E_1	E_2
$I_0(r) = \{(S^{in}, D) : \max\{r(f(S^{in}) - a), (1-r)(f(S^{in}) - a)\} \leq D\}$	GAS		
$I_1(r) = \{(S^{in}, D) : r(f(S^{in}) - a) \leq D$ and $D < (1-r)(f(S^{in}) - a)\}$	U	GAS	
$I_2(r) = \{(S^{in}, D) : 0 < D < \min\{r(f(S^{in}) - a), (1-r)(f(S^{in}) - a)\}\}$	U	U	GAS
$I_3(r) = \{(S^{in}, D) : (1-r)(f(S^{in}) - a) \leq D$ and $D < r(f(S^{in}) - a))\}$	U		GAS

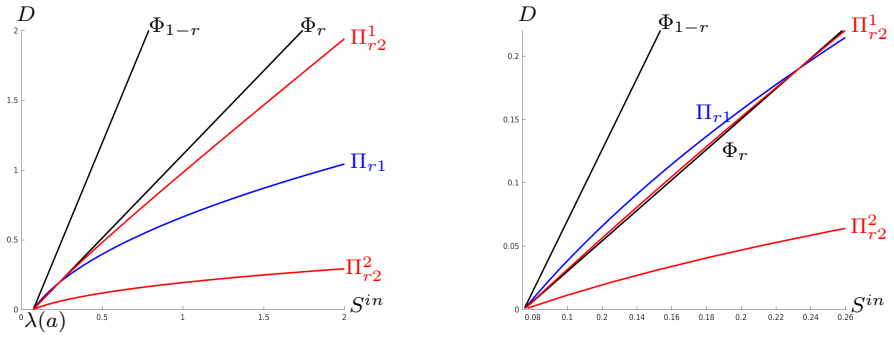

(a) $r = 0.3$ (b) Zoom of (a)

FIGURE 13. (a) The operating diagram for $f(S) = 4S$, $a = 0.3$ showing curves Φ_r and Φ_{1-r} (in black), Π_{r1} (in blue), Π^1_{r2} and Π^2_{r2} (in red). (b): A zoom showing the intersection point of Φ_r, Π_{r1} and Π^1_{r2}.

Proposition 17. *Apart from point* $(\lambda(a), 0)$*, curves* Π_{r1} *and* Φ_r *can intersect at a positive point if and only if* $0 < r < \frac{3-\sqrt{5}}{2}$*. The intersection point is* $(p_1(D_0, r), D_0)$*, where* $D_0 = \frac{1-3r+r^2}{r}a$*.*

Proof. The equation (21) giving the intersection points of Π_{r1} and Φ_r curves is equivalent to the algebraic equation

$$D\left(-a + 3ra + Dr - r^2 a\right) = 0.$$

Therefore, apart from $D = 0$ which corresponds to the intersection point $(\lambda(a), 0)$ of Π_{r1} and Φ_r, these curves can intersect at point $(p_1(D_0, r), D_0)$, where $D_0 = \frac{1-3r+r^2}{r}a$. This value of D is in the domain of definition of the function $D \mapsto p_1(D, r)$, which is $[0, +\infty)$, if and only if $D \geq 0$, that is, $0 < r < \frac{3-\sqrt{5}}{2}$. □

TABLE 6. f linear

$f(S)$	$=$	γS
$\lambda(D)$	$=$	D/γ
$p_1(D, r)$	$=$	$\frac{(D+a)(D+a(1-r))}{a(1-r)\gamma}$
$\pi_1(D)$	$=$	$\frac{(D+a)^2}{a\gamma}$
$r_0(S^{in}, D)$	$=$	$\frac{D}{\gamma S^{in} - a}$
$r_1(S^{in}, D)$	$=$	$\frac{(D+a)^2 - a\gamma S^{in}}{a(D+a-\gamma S^{in})}$
$p_2^1(D, r)$	$=$	$\frac{D+a}{2\gamma r(1-r)a^2}\left(D^2 + 2aD + 2a^2 r(1-r) - D\sqrt{D^2 + 4aD + 4a^2 r}\right)$
$p_2^2(D, r)$	$=$	$\frac{D+a}{2\gamma r(1-r)a^2}\left(D^2 + 2aD + 2a^2 r(1-r) + D\sqrt{D^2 + 4aD + 4a^2 r}\right)$
$\pi(D)$	$=$	$\frac{2(D+a)^2}{\gamma(D+2a)}$

The functions p_2^1 and p_2^2 which are defined implicitly as solutions of the equation $f_1 = h_1$, can be given explicitly, as shown in the following proposition.

Proposition 18. *The functions* p_2^1 *and* p_2^2 *are given explicitly by the formulas in Table 6.*

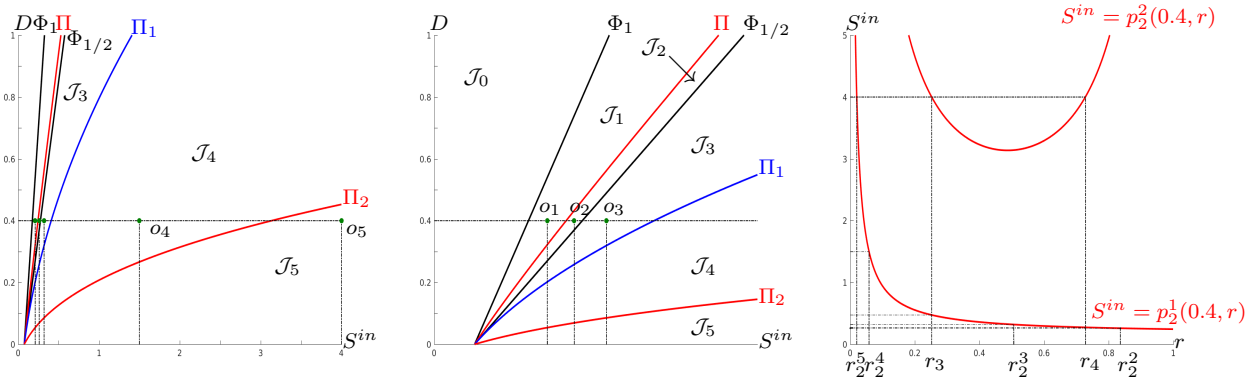

(a) (b): Zoom of (a) (c)

FIGURE 14. (a) and (b): The curves Φ_1, $\Phi_{1/2}$ (in black), Π_1 (in blue), Π and Π_2 (in red) divide the operating plane in six regions, $\mathcal{J}_k$, $k = 0..5$ and the operating points $o_k \in \mathcal{J}_k$, $k = 1..5$. (c): The graphical depiction of Assumptions 6 and 7, for $D = 0.4$, showing the values $r_2^k = r_2(S^{in}, D)$, corresponding to o_k, $k = 2..5$, respectively, and the values of r_3 and r_4 corresponding to o_5. The operating points are $o_1 = (0.21, 0.4)$, $o_2 = (0.26, 0.4)$, $o_3 = (0.32, 0.4)$, $o_4 = (1.5, 0.4)$ and $o_5 = (4, 0.4)$.

Proof. The equation $f(S_2) = h_2(S_2)$ is equivalent to the algebraic quadratic equation

$$c_2 S_2^2 - c_1 S_2 + c_0 = 0,$$

with c_i, $i = 0, 1, 2$ defined by

$$c_2 = \gamma^2(D + ra), \quad c_1 = \gamma(D^2 + 2aD + 2a^2 r), \quad c_0 = a^2(D + ra). \tag{46}$$

The discriminant is positive:

$$\Delta := c_1^2 - 4c_2 c_0 = D^2\gamma^2(D^2 + 4aD + 4a^2 r). \tag{47}$$

As c_i, $i = 0, 1, 2$ and Δ are positive then $f(S_2) = h_2(S_2)$ admits two positive solutions that are explicitly defined by:

$$S_2^1(D) = \frac{D^2+2aD+2a^2r-D\sqrt{D^2+4aD+4a^2r}}{2\gamma(D+ra)}, \quad S_2^2(D) = \frac{D^2+2aD+2a^2r+D\sqrt{D^2+4aD+4a^2r}}{2\gamma(D+ra)}.$$

One deduces the expressions of $p_2^1(D, r)$ and $p_2^2(D, r)$ by using (29). □

Proposition 19. *For all $D > 0$, we have $\pi(D) < \lambda(2D + a) < \pi_1(D)$.*

Proof. The condition $\pi(D) < \lambda(2D + a)$ is equivalent to $\frac{2(D+a)^2}{D+2a} < 2D + a$, which is equivalent to $2(D + a)^2 < (D + 2a)(2D + a)$, which is equivalent to $aD > 0$.
The condition $\lambda(2D + a) < \pi_1(D)$ is equivalent to $2D + a < \frac{(D+a)^2}{a}$, which is equivalent to $(2D + a)a < 2(D + a)^2$, which is true, since $D > 0$. □

Remark 10. From Proposition 19 it is seen that $\Phi_{1/2}$ lies to the right of Π and to the left of Π_1. This property complements the one given in Remark 7. The relative position of curve Π_2 (which is only known to be to the right of curve Π) in relation to the other curves, gives a complete description of all possible cases.

In Figure 14, it is assumed that $f(S) = 4S$ and $a = 0.3$, as in Figure 13, and the curve Π_2 is represented numerically, as well as curves Φ_1, $\Phi_{1/2}$, Π_1 and Π, see Figure 14 (a), (b). It can be seen that curve Π_2 lies to the right of curve Π_1. Therefore these curves divide the operating plane in six regions labeled $\mathcal{J}_k$, $k = 0..5$. Let us illustrate the behavior of the productivities $P_1(S^{in}, D, r)$ and $P_2(S^{in}, D, r)$, as a function of r, for the operating points $o_k \in \mathcal{J}_k$, $k = 0..5$, shown in Figure 14 (a), (b).

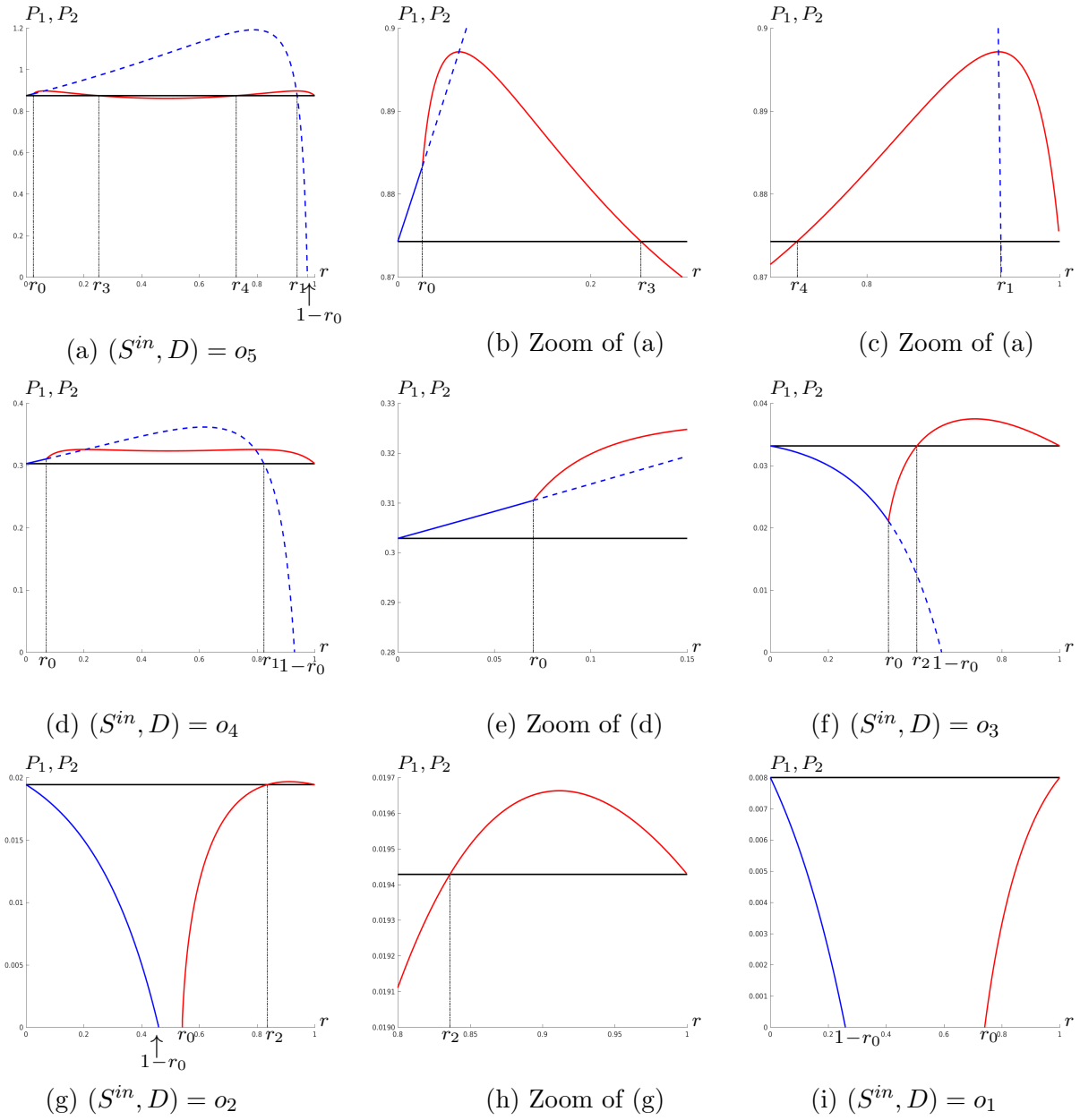

(a) $(S^{in}, D) = o_5$ (b) Zoom of (a) (c) Zoom of (a)

(d) $(S^{in}, D) = o_4$ (e) Zoom of (d) (f) $(S^{in}, D) = o_3$

(g) $(S^{in}, D) = o_2$ (h) Zoom of (g) (i) $(S^{in}, D) = o_1$

FIGURE 15. The curves of the functions $r \mapsto P_2(S^{in}, D, r)$ (in red) and $r \mapsto P_1(S^{in}, D, r)$ (in blue), for S^{in} and D fixed and the corresponding value of $P(S^{in}, D)$ (in black). The r_k, $k = 0, \ldots, 4$ values are given in Table 7.

TABLE 7. The values of r_k, corresponding to the operating points $o_1, \ldots, o_5$ in Figure 14.

	r_0	r_1	r_2	r_3	r_4
$o_5 = (4, 0.4)$	$0.255\,10^{-1}$	0.939	$0.203\,10^{-1}$	0.252	0.728
$o_4 = (1.5, 0.4)$	$0.702\,10^{-1}$	0.824	$0.583\,10^{-1}$		
$o_3 = (0.32, 0.4)$	0.408		0.506		
$o_2 = (0.26, 0.4)$	0.541		0.836		
$o_1 = (0.21, 0.4)$	0.741				

Figure 14(c) shows the functions $r \mapsto p_2^1(D, r)$ and $r \mapsto p_2^2(D, r)$, for $D = 0.4$ corresponding to the horizontal line $D = 0.4$ depicted in panels (a), (b) of the figure. It appears that $r \mapsto p_2^1(D, r)$ is decreasing and $r \mapsto p_2^2(D, r)$ is decreasing and then increasing. Therefore the Assumptions

6 and 7 are satisfied for $f(S) = 4S$, $a = 0.3$ and $D = 0.4$. Figure 14(c) shows the values of $r_2(S^{in}, D)$ corresponding to the four operating points o_k, $k = 2, 3, 4, 5$ depicted in panels (a) and (b). The figure shows also the values of $r_3(S^{in}, D)$ and $r_4(S^{in}, D)$ corresponding to $o_5 = (4, 0.4)$. The numerical values of r_2, r_3 and r_4, with two digits are collected in Table 7. This table gives also $r_0(S^{in}, D)$ and $r_1(S^{in}, D)$, whose expressions are known analytically, see Table 6.

Figure 15 shows $P_1(S^{in}, D, r)$ and $P_2(S^{in}, D, r)$, as functions of r, for the five operating points o_k, $k = 1..5$ shown in Figure 14 (a), (b). Let us first recall the theoretical predictions. Since $o_5 = (4, 0.4) \in \mathcal{J}_5$, this operating point satisfies the condition $S^{in} > \pi_2(D) > \pi_1(D)$. Hence, from Proposition 7 it is deduced that $P_1(4, 0.4, r) > P(4, 0.4)$ if and only if $0 < r < r_1$. Moreover, from Proposition 9 it is deduced that $P_2(4, 0.4, r) > P(4, 0.4)$ if and only if $r_0 = \max(r_0, r_2) < r < r_3$ or $r_4 < r < 1$. This behavior is illustrated in Figure 15(a), the zoom in panel (b) showing the values r_0 and r_3, and the zoom in panel (c), showing the values r_4 and r_1.

On the other hand, since $o_4 = (1.5, 0.4) \in \mathcal{J}_4$, this operating point satisfies the condition $\pi_2(D) > S^{in} > \pi_1(D) > \pi(D)$. Hence, from Proposition 7 it is deduced that $P_1(1.5, 0.4, r) > P(1.5, 0.4)$ if and only if $0 < r < r_1$. Moreover, from Proposition 9 it is deduced that $P_2(1.5, 0.4, r) > P(1.5, 0.4)$ if and only if $r_0 = \max(r_0, r_2) < r < 1$. This behavior is illustrated in Figure 15(d) and the zoom in panel (e), showing the value r_0.

Since $o_3 = (0.32, 0.4) \in \mathcal{J}_3$, this operating point satisfies the condition $\pi_1(D) > S^{in} > \lambda(2D+a) > \pi(D)$. Hence, from Proposition 7 it is deduced that $P_1(0.32, 0.4, r) < P(0.32, 0.4)$ for any $r \in (0, 1-r_0)$. Moreover, from Proposition 9 it is deduced that $P_2(0.32, 0.4, r) > P(0.32, 0.4)$ if and only if $r_2 = \max(r_0, r_2) < r < 1$. This behavior is illustrated in Figure 15(f), showing the values r_0, r_2 and $1 - r_0$.

Since $o_2 = (0.26, 0.4) \in \mathcal{J}_2$, this operating point satisfies the condition $\pi_1(D) > \lambda(2D + a) > S^{in} > \pi(D)$. Hence, from Proposition 7 it is deduced that $P_1(0.26, 0.4, r) < P(0.26, 0.4)$ for any $r \in (0, 1 - r_0)$. Moreover, from Proposition 9 it is deduced that $P_2(0.26, 0.4, r) > P(0.26, 0.4)$ if and only if $r_2 = \max(r_0, r_2) < r < 1$. This behavior is illustrated in Figure 15(g), showing the values $1 - r_0$, r_0 and r_2 and the zoom in panel (h), showing the value r_2.

Finally, since $o_1 = (0.21, 0.4) \in \mathcal{J}_1$, this operating point satisfies the condition $\pi_1(D) > \lambda(2D+a) > S^{in} > \pi(D)$. Hence, from Proposition 7 it is deduced that $P_1(0.21, 0.4, r) < P(0.21, 0.4)$ for any $r \in (0, 1-r_0)$. Moreover, from Proposition 9 it is deduced that $P_2(0.21, 0.4, r) < P(0.21, 0.4)$ for any $r_0 < r < 1$. This behavior is illustrated in Figure 15 (i), showing the values $1 - r_0$ and r_0.

Recall that when $r_0 < 1/2$, it corresponds to a transcritical bifurcation of E_2 and E_1, while when $r_0 > 1/2$, it corresponds to a transcritical bifurcation of E_2 and E_0. The first case can be seen in Figures 15 (a), (b), (d), (e) and (f) and the second case can be seen in Figures 15 (g), (i). Recall also that $1 - r_0$ corresponds to a transcritical bifurcation of E_1 and E_0, which is observed in 15 (a), (d), (f), (g) and (i).

Remark 11. When a tends to 0, curves Π_1 and Π_2 tend towards the S^{in}-axis while curves Π and $\Phi_{1/2}$ tend towards each other. Therefore, in the limiting case $a = 0$, there are only the regions J_0, J_1 and J_3, bounded by curves Φ_1 and $\Phi_{1/2}$. This result is in agreement with the results obtained in the no mortality case, see Section 5.1 of [2].

Figure 15 shows that for the operating points o_5 and o_4 the most efficient device is obtained for $r_1^{opt}(o_5) \approx 0.789$ and $r_1^{opt}(o_4) \approx 0.616$. For these operating points, the maximum of the productivity is obtained for the unstable steady state E_1. On the other hand, for the operating points o_3 and o_2, the most efficient device is obtained for $r_2^{opt}(o_3) \approx 0.707$, $r_2^{opt}(o_2) \approx 0.912$. For these operating points, the productivity of the serial device is obtained with the coexistence steady state E_2.

C.2. **Hill growth functions.** In this section we apply our results to the Hill growth function $f(S) = mS^p/(K^p+S^p)$. Note that $m = \sup_{S>0} f(S)$. Since $f'(S) = mpK^pS^{p-1}/(K^p+S^p)^2 > 0$, f satisfies Assumption 1. Moreover, it was proved in Section 5.3 of [3], that for the Hill function, $f_a''(S) > 0$ for all $a \geq 0$ and all $S > \lambda(a)$, where $f_a(S) = 1/(f(S)-a)$. Then using the Proposition 11, it is seen that Assumptions 2 and 5 are satisfied. Finally, it was also proved in Section 5.3

of [3] that, for the Hill function,

$$f'\left(\lambda\left(\frac{D}{r}+a\right)\right) < \frac{1}{r}f'(\lambda(D+a)), \qquad \text{for all } r \in (0,1).$$

Replacing r by $1-r$, it is deduced that (48) is satisfied. Hence, using the Lemma 12 in Appendix D.1, one deduces that Assumption 3 is satisfied. As for linear and Monod functions, Assumptions 4, 6 and 7 will be checked graphically.

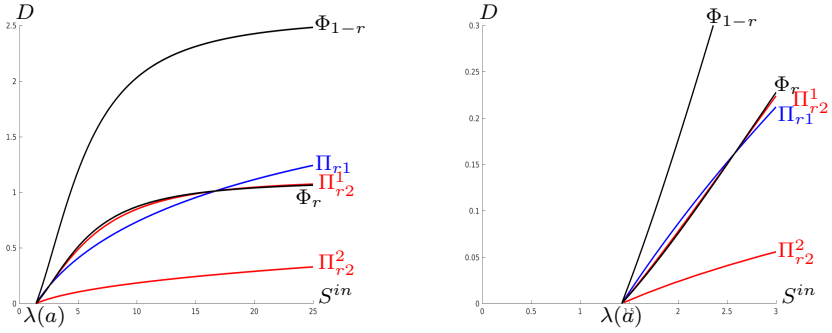

(a) $r = 0.3$ (b) Zoom of (a)

FIGURE 16. (a) The operating diagram for $f(S) = 4S^2/(25+S^2)$, $a = 0.3$ showing curves Φ_r and Φ_{1-r} (in black), Π_{r1} (in blue), Π^1_{r2} and Π^2_{r2} (in red). (b): A zoom showing the first intersection point of Φ_r, Π_{r1} and Π^1_{r2}. (c): A zoom showing the second intersection point of Φ_r, Π_{r1} and Π^1_{r2}.

TABLE 8. f Hill

$f(S)$	$=$	$\frac{mS^p}{K^p+S^p}$
$\lambda(D)$	$=$	$K\left(\frac{D}{m-D}\right)^{\frac{1}{p}}$
$p_1(D,r)$	$=$	$\frac{K}{ar}\left((D+a)\left(\frac{D+a(1-r)}{(m-a)(1-r)-D}\right)^{\frac{1}{p}} - (D+(1-r)a)\left(\frac{D+a}{m-D-a}\right)^{\frac{1}{p}}\right)$
$\pi_1(D)$	$=$	$K\frac{(m-pa)D+pa(m-a)}{pa(D+a)}\left(\frac{D+a}{m-D-a}\right)^{\frac{1}{p}+1}$
$\pi(D)$	$=$	$K\frac{-pD^2+(m(p+1)-3pa)D+2pa(m-a)}{p(D+2a)(D+a)}\left(\frac{D+a}{m-D-a}\right)^{\frac{1}{p}+1}$
$r_0(S^{in},D)$	$=$	$\frac{D(K^p+S^{inp})}{mS^{inp}-a(K^p+S^{inp})}$

TABLE 9. The values of r_k, corresponding to the operating points $o_1,\dots,o_6$ in Figure 17.

	r_0	r_1	r_2	r_3	r_4
$o_6 = (48, 1.9)$	0.520	$0.530\,10^{-1}$	0.527		
$o_5 = (20, 0.2)$	$0.577\,10^{-1}$	0.936	$0.542\,10^{-1}$	0.119	0.860
$o_4 = (20, 0.9)$	0.260	0.518	0.255		
$o_3 = (7, 0.9)$	0.383		0.450		
$o_2 = (20, 1.9)$	0.548		0.609		
$o_1 = (7, 1.9)$	0.809				

In Figure 17, it is assumed that $f(S) = 4^2S/(5^2+S)$ and $a = 0.3$, and the curve Π_2 is represented numerically, as well as curves Φ_1, $\Phi_{1/2}$, Π_1 and Π, see Figure 17 (a) and (b). It can be seen that curve Π_2 lies to the right of curve Π_1 and $\Phi_{1/2}$. Therefore these curves divide the operating plane in seven regions labeled $\mathcal{J}_k$, $k = 0..6$. Let us illustrate the behavior of the productivities $P_1(S^{in}, D, r)$ and $P_2(S^{in}, D, r)$, as a function of r, for the operating points $o_k \in \mathcal{J}_k$, $k = 0..6$, shown in Figure 17 (a) and (b).

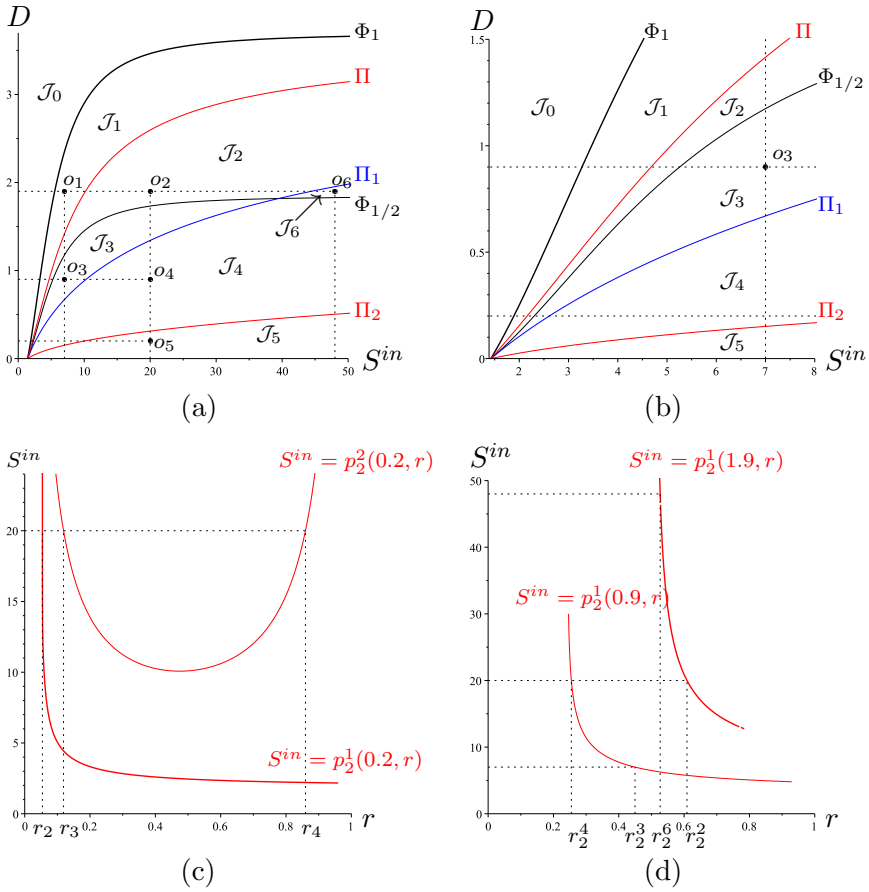

FIGURE 17. (a) and (b): The curves Φ_1, $\Phi_{1/2}$ (in black), Π_1 (in blue), Π and Π_2 (in red) divide the operating plane in seven regions, $\mathcal{J}_k$, $k = 0..6$ and the operating points $o_k \in \mathcal{J}_k$, $k = 1..6$. (c): The graphical depiction of Assumptions 6 and 7, for $D = 0.2$, showing the values $r_2 = r_2(S^{in}, D)$, $r_3 = r_3(S^{in}, D)$ and $r_4 = r_4(S^{in}, D)$, corresponding to o_5. (d): The graphical depiction of Assumption 6, for $D = 0.9$ and $D = 1.9$, showing the values $r_2^k = r_2(S^{in}, D)$, corresponding to o_k, $k = 2, 3, 4, 6$, respectively. The operating points are $o_1 = (8, 1.9)$, $o_2 = (20, 1.9)$, $o_3 = (8, 0.9)$, $o_4 = (20, 0.9)$, $o_5 = (20, 0.2)$. and $o_6 = (48, 1.9)$.

Figure 17 (c) shows the function $r \mapsto p_2^1(D, r)$ and $r \mapsto p_2^2(D, r)$, for $D = 0.2$, corresponding to the horizontal line $D = 0.2$ depicted in panels (a) and (b) of the figure. It appears that $r \mapsto p_2^1(D, r)$ is decreasing and $r \mapsto p_2^2(D, r)$ is decreasing and then increasing. Therefore the Assumptions 6 and 7 are satisfied. Figure 17 (c) shows the values of $r_2(S^{in}, D)$, $r_3(S^{in}, D)$ and $r_4(S^{in}, D)$ corresponding to $o_5 = (20, 0.2)$. Figure 17 (d) shows the functions $r \mapsto p_2^1(D, r)$ for $D = 0.9$ and $D = 1.9$, corresponding to the horizontal lines $D = 0.9$ and $D = 1.9$ depicted in panels (a) and (b) of the figure. It appears that $r \mapsto p_2^1(D, r)$ is decreasing. Therefore the Assumption 6 is satisfied. Figure 17(d) shows the values of $r_2(S^{in}, D)$ corresponding to the two operating points o_k, $k = 2, 3, 4, 6$ depicted in panels (a) and (b). The numerical values of r_0, r_1, r_2, r_3 and r_4, with three digits are collected in Table 9. Figure 18 shows $P_1(S^{in}, D, r)$ and $P_2(S^{in}, D, r)$, as functions of r, for the six operating points o_k, $k = 1..6$ shown in Figure 17 (a) and (b). Let us first recall the theoretical predictions.

Since $o_6 = (48, 1.9) \in \mathcal{J}_6$, this operating point satisfies the condition $\pi_2(D) > \lambda(2D + a) > S^{in} > \pi_1(D) > \pi(D)$. Hence, from Proposition 7 it is deduced that $P_1(48, 1.9, r) > P(48, 1.9)$ if and only if $0 < r < r_1$. Moreover, from Proposition 9 it is deduced that $P_2(48, 1.9, r) > P(48, 1.9)$

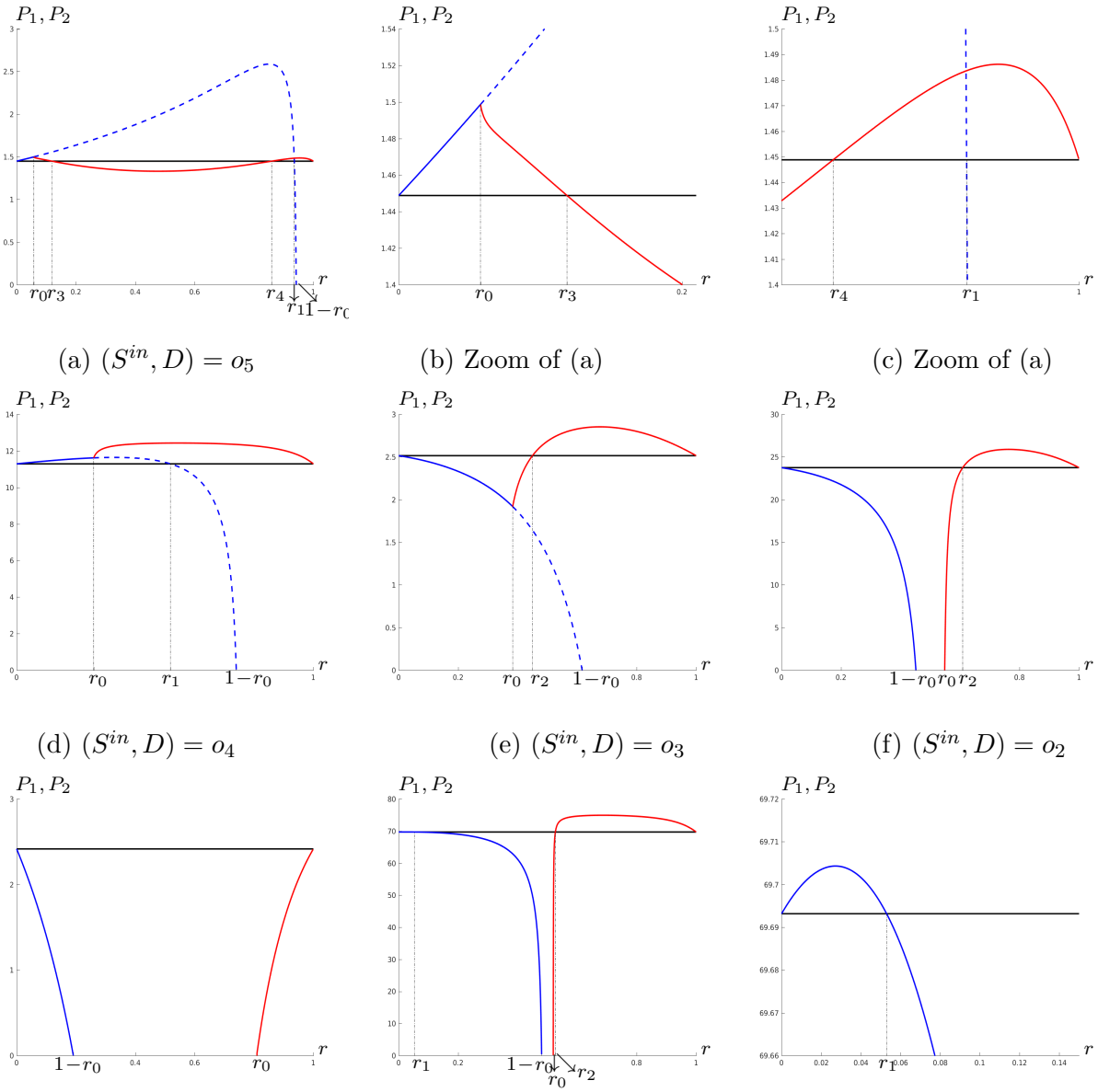

(a) $(S^{in}, D) = o_5$ (b) Zoom of (a) (c) Zoom of (a)

(d) $(S^{in}, D) = o_4$ (e) $(S^{in}, D) = o_3$ (f) $(S^{in}, D) = o_2$

(g) $(S^{in}, D) = o_1$ (h) $(S^{in}, D) = o_6$ (i) Zoom of (h)

FIGURE 18. The curves of the functions $r \mapsto P_2(S^{in}, D, r)$ (in red) and $r \mapsto P_1(S^{in}, D, r)$ (in blue), for S^{in} and D fixed and the corresponding value of $P(S^{in}, D)$ (in black). The r_k, $k = 0, \ldots, 4$ values are given in Table 9.

if and only if $r_2 = \max(r_0, r_2) < r < 1$. This behavior is illustrated in Figure 9 (h), showing the values r_1, $1 - r_0$, r_0 and r_2 and the zoom in panel (i) showing the value r_1.

Similarly, since $o_5 = (20, 0.2) \in \mathcal{J}_5$, this operating point satisfies the condition $S^{in} > \pi_2(D) > \pi_1(D)$. Hence, from Proposition 7 it is deduced that $P_1(20, 0.2, r) > P(20, 0.2)$ if and only if $0 < r < r_1$. Moreover, from Proposition 9 it is deduced that $P_2(20, 0.2, r) > P(20, 0.2)$ if and only if $r_0 = \max(r_0, r_2) < r < r_3$ or $r_4 < r < 1$. This behavior is illustrated in Figure 18 (a), the zoom in panel (b) showing the values r_0 and r_3, and the zoom in panel (c), showing the values r_4 and r_1.

On the other hand, since $o_4 = (20, 0.9) \in \mathcal{J}_4$, this operating point satisfies the condition $\pi_2(D) > S^{in} > \pi_1(D) > \pi(D)$. Hence, from Proposition 7 it is deduced that $P_1(20, 0.9, r) > P(20, 0.9)$ if and only if $0 < r < r_1$. Moreover, from Proposition 9 it is deduced that $P_2(20, 0.9, r) > P(20, 0.9)$ if and only if $r_0 = \max(r_0, r_2) < r < 1$. This behavior is illustrated in Figure 18(d).

Since $o_3 = (7, 0.9) \in \mathcal{J}_3$, this operating point satisfies the condition $\pi_1(D) > S^{in} > \lambda(2D + a) > \pi(D)$. Hence, from Proposition 7 it is deduced that $P_1(7, 0.9, r) < P(7, 0.9)$ for any $r \in (0, 1 - r_0)$. Moreover, from Proposition 9 it is deduced that $P_2(7, 0.9, r) > P(7, 0.9)$ if and only if $r_2 = \max(r_0, r_2) < r < 1$. This behavior is illustrated in Figure 9(e), showing the values r_0, r_2 and $1 - r_0$.

Since $o_2 = (20, 1.9) \in \mathcal{J}_2$, this operating point satisfies the condition $\pi_1(D) > \lambda(2D + a) > S^{in} > \pi(D)$. Hence, from Proposition 7 it is deduced that $P_1(20, 1.9, r) < P(20, 1.9)$ for any $r \in (0, 1 - r_0)$. Moreover, from Proposition 9 it is deduced that $P_2(20, 1.9, r) > P(20, 1.9)$ if and only if $r_2 = \max(r_0, r_2) < r < 1$. This behavior is illustrated in Figure 18 (f), showing the values $1 - r_0$, r_0 and r_2.

Finally, since $o_1 = (7, 1.9) \in \mathcal{J}_1$, this operating point satisfies the condition $\pi_1(D) > \lambda(2D + a) > S^{in} > \pi(D)$. Hence, from Proposition 7 it is deduced that $P_1(7, 1.9, r) < P(7, 1.9)$ for any $r \in (0, 1 - r_0)$. Moreover, from Proposition 9 it is deduced that $P_2(7, 1.9, r) < P(7, 1.9)$ for any $r_0 < r < 1$. This behavior is illustrated in Figure 18 (g), showing the values $1 - r_0$ and r_0.

Recall that when $r_0 < 1/2$, then r_0 corresponds to a transcritical bifurcation of E_2 and E_1, while when $r_0 > 1/2$, then r_0 corresponds to a transcritical bifurcation of E_2 and E_0. The first case can be seen in Figure 18 (a), (b), (d) and (e), and the second case can be seen in Figure 18 (g), (h) and (i). Recall also that $1 - r_0$ corresponds to a transcritical bifurcation of E_1 and E_0, which is observed in 18 (a), (d), (e), (f), (g) and (h).

Figure 18 shows that for the operating point o_5 the most efficient device is obtained for $r_1^{opt}(o_5) \approx 0.851$. For these operating points, the maximum of the productivity is obtained for the unstable steady state E_1. On the other hand, for the operating points o_4, o_3, o_2 and o_6, the most efficient device is obtained for $r_2^{opt}(o_4) \approx 0.544$, $r_2^{opt}(o_3) \approx 0.676$, $r_2^{opt}(o_2) \approx 0.764$ and $r_2^{opt}(o_6) \approx 0.687$. For these operating points, the productivity of the serial device is obtained with the coexistence steady state E_2.

Appendix D. Proofs

D.1. **Preliminary lemmas.** We give some lemmas that provide sufficient conditions for our assumptions to be satisfied. The following lemma provides sufficient conditions for Assumption 2 to be satisfied.

Lemma 11. *Assumption 2 is satisfied for any increasing concave function f. It is satisfied also for any increasing function f, such that $1/f$ is convex.*

Proof. Assume that f is concave. Since h_2 defined by (27) is strictly convex and increasing, its graph can intersect the graph of the increasing concave function f in at most two points.
Assume now that $1/f$ is convex. The equation $h_2(S_2) = f(S_2)$ is equivalent to the equation $\frac{1}{h_2(S_2)} = \frac{1}{f(S_2)}$. Since $1/h_2$ is strictly concave and decreasing, its graph can intersect the graph of the decreasing convex function $1/f$ in at most two points. In both cases, from Lemma 2 one knows that there exists at least two intersection points. Therefore, we have exactly two intersection points. □

The following Lemma provides a sufficient condition for Assumption 3 to be satisfied.

Lemma 12. *Assume that*

$$f'\left(\lambda\left(\tfrac{D}{1-r} + a\right)\right) \leq \tfrac{1}{1-r} f'\left(\lambda\left(D + a\right)\right) \tag{48}$$

then $\frac{\partial p_1}{\partial D}(D, r) > 0$. If f' is decreasing, then the condition (48) is satisfied.

Proof. From (17) we deduce that

$$\tfrac{\partial p_1}{\partial D}(D, r) = \lambda'(D + a) + \tfrac{D+a}{ra}\left(\tfrac{1}{1-r}\lambda'\left(\tfrac{D}{1-r} + a\right) - \lambda'(D + a)\right) + \tfrac{1}{ra}\left(\lambda\left(\tfrac{D}{1-r} + a\right) - \lambda(D + a)\right).$$

Notice that $\lambda'(D + a) > 0$ and $\lambda\left(\frac{D}{1-r} + a\right) - \lambda(D + a) > 0$. Therefore the condition

$$\tfrac{1}{1-r}\lambda'\left(\tfrac{D}{1-r} + a\right) - \lambda'(D + a) \geq 0$$

is sufficient to have $\frac{\partial p_1}{\partial D}(D,r) > 0$. Using $\lambda'(D) = 1/f'(\lambda(D))$, this condition is equivalent to (48). Note that if f' is decreasing, then this condition is satisfied. Indeed, we have

$$f'\left(\lambda\left(\tfrac{D}{1-r}+a\right)\right) \leq f'\left(\lambda\left(D+a\right)\right) < \tfrac{1}{1-r} f'\left(\lambda\left(D+a\right)\right)$$

which is the condition (48). □

The following lemma provides a sufficient condition for Assumption 5 to be satisfied.

Lemma 13. *Let $D \in [0, m-a)$ and l_D be defined on $\mathrm{dom}(l_D) := \left[0, 1-\frac{D}{m-a}\right)$ by $l_D(r) := \lambda\left(\frac{D}{1-r}+a\right)$. The following conditions are equivalent.*

a: *For all $(D,r) \in \mathrm{dom}(p_1)$, $\frac{\partial p_1}{\partial r}(D,r) > 0$.*
b: *For all $(D,r) \in \mathrm{dom}(p_1)$, $l_D(r) < l_D(0) + r l'_D(r)$.*

*If, for $D \in (0, m-a)$, l_D is strictly convex on $\mathrm{dom}(l_D)$, then the condition **b** is satisfied.*
If f is twice derivable, then l_D is twice derivable and the following conditions are equivalent.

1: *For all $D \in (0, m-a)$ and $r \in \mathrm{dom}(l_D)$, $l''_D(r) > 0$.*
2: *For all $S > \lambda(a)$, $(f(S)-a)f''(S) < 2\left(f'(S)\right)^2$.*
3: *For all $S > \lambda(a)$, $f''_a(S) > 0$, where $f_a(S)$ is defined by (40).*

Proof. Notice first that, from (17), $p_1(D,r)$ can be written

$$p_1(D,r) = l_D(0) + \tfrac{D+a}{ra}\left(l_D(r) - l_D(0)\right).$$

The partial derivative, with respect to r of p_1 is given then by

$$\frac{\partial p_1}{\partial r}(D,r) = -\tfrac{D+a}{ar^2}\left(l_D(r) - l_D(0)\right) + \tfrac{D+a}{ra} l'_D(r). \tag{49}$$

Therefore $\frac{\partial p_1}{\partial r}(D,r) > 0$ if and only if $l_D(r) < l_D(0) + r l'_D(r)$. This proves the equivalence of the conditions **a** and **b** of the lemma.

Assume that l_D is strictly convex. For all s and r in $\mathrm{dom}(l_D)$, if $s \neq r$, then

$$l_D(s) > l_D(r) + (s-r) l'_D(r).$$

Taking $s = 0$ and $r \in (0, 1 - D/(m-a))$ one obtains **b**. Assume now that f is twice derivable. Then, so is l_D. Using

$$\lambda'(D) = \tfrac{1}{f'(\lambda(D))} \quad \text{and} \quad \lambda''(D) = -\tfrac{f''(\lambda(D))}{(f'(\lambda(D)))^3},$$

we can write

$$\begin{aligned} l''_D(r) &= \tfrac{2D}{(1-r)^3}\lambda'\left(\tfrac{D}{1-r}+a\right) + \tfrac{D^2}{(1-r)^4}\lambda''\left(\tfrac{D}{1-r}+a\right) \\ &= \tfrac{D}{(1-r)^3\left(f'\left(\lambda\left(\frac{D}{1-r}+a\right)\right)\right)^3}\left(2\left(f'\left(\lambda\left(\tfrac{D}{1-r}+a\right)\right)\right)^2 - \tfrac{D}{1-r} f''\left(\lambda\left(\tfrac{D}{1-r}+a\right)\right)\right). \end{aligned}$$

Therefore, the condition **1** in the lemma is equivalent to the following condition: For all $D \in (0, m-a)$ and $r \in [0, 1 - D/(m-a))$,

$$\tfrac{D}{1-r} f''\left(\lambda\left(\tfrac{D}{1-r}+a\right)\right) < 2 f'\left(\lambda\left(\tfrac{D}{1-r}+a\right)\right)^2. \tag{50}$$

Using the notation $S = \lambda\left(\frac{D}{1-r}+a\right)$, which is the same as $\frac{D}{1-r} = f(S) - a$, the condition (50) is equivalent to : For all $S > 0$, $(f(S)-a)f''(S) < 2\left(f'(S)\right)^2$, which is the condition **2** in the lemma. This proves the equivalence of the conditions **1** and **2** of the lemma. Straightforward computation shows that

$$f''_a(S) = \tfrac{2f'(S)^2 - f''(S)(f(S)-a)}{(f(S)-a)^3}.$$

Hence, $f''_a(S) > 0$ if and only if $(f(S)-a)f''(S) < 2f'(S)^2$, which proves the equivalence of the conditions **2** and **3** of the lemma. □

D.2. **Proof of Proposition 11.** If $f'' \leq 0$, then f is concave and by Lemma 11, Assumption 2 is satisfied. Moreover, f' is decreasing and, by Lemma 12, $\frac{\partial p_1}{\partial D} > 0$, so that Assumption 3 is satisfied. Finally, the condition **2** in Lemma 13 is satisfied, which is equivalent to the fact that $l''_D(r) > 0$. Therefore l_D is strictly convex, which, according to the lemma, implies that $\frac{\partial p_1}{\partial r} > 0$, so that Assumption 5 is satisfied.

If $f''_a > 0$ for any $a \geq 0$, then $f_0 = 1/f$ is (strictly) convex and by Lemma 11, Assumption 2 is satisfied. Moreover, the condition **3** in Lemma 13 is satisfied, which is equivalent to the fact that $l''_D(r) > 0$. Therefore l_D is strictly convex, which, according to the lemma, implies that $\frac{\partial p_1}{\partial r} > 0$, so that Assumption 5 is satisfied.

D.3. **Proof of Proposition 12.** The equation (21) giving the intersection points of Π_{r1} and Φ_r curves is equivalent to the algebraic equation

$$D\left(D^2 - bD + c\right) = 0, \quad \text{where} \quad b = r(m-2a), \quad c = a(m-a)(r^2-3r+1).$$

Therefore, apart from $D = 0$ which corresponds to the intersection point $(\lambda(a), 0)$ of Π_{r1} and Φ_r, these curves can intersect at points $Q_i = (p_1(d_i, r), d_i)$, where d_i, $i = 1, 2$, are the solutions of equation $D^2 - bD + c = 0$, i.e. $d_1 = \frac{b+\sqrt{\Delta}}{2}$ and $d_2 = \frac{b-\sqrt{\Delta}}{2}$, where $\Delta = b^2 - 4c$. This proves the formulas for d_1 and d_2 given in the proposition. The roots d_1 and d_2 correspond to an intersection point whenever they are real and satisfy $0 < d_2 \leq d_1 < (1-r)(m-a)$, i.e. $(d_i, r) \in \mathrm{dom}(p_1)$, $i = 1, 2$. A necessary condition for this to be true is that $r < 1/2$. Note that when $r = 1/2$ then $d_1 = \frac{m-a}{2}$ and $d_2 < 0$. This result is in agreement with Proposition 3 which states that there is no intersection when $r \in [1/2, 1)$. Therefore we must restrict our attention to $r \in (0, 1/2)$.

We obtain the signs of the roots of the polynomial of degree 2 in D by considering the signs of its coefficients b and c and that of its discriminant Δ. First, note that b is positive if and only if $a < m/2$ and c is negative if and only if $r^2 - 3r + 1 > 0$, i.e. $\frac{3-\sqrt{5}}{2} < r < \frac{1}{2} < \frac{3+\sqrt{5}}{2}$. On the other hand, the discriminant Δ is written

$$\Delta = (8a^2 - 8am + m^2)r^2 + 12a(m-a)r - 4a(m-a).$$

The reduced discriminant of Δ, considered as a polynomial of degree 2 in r, is given by

$$36a^2(m-a)^2 + 4a(m-a)(8a^2 - 8am + m^2) = 4\Delta_1 > 0,$$

where Δ_1 is defined in the proposition. Therefore $\Delta = 0$ if and only if $r = r_1$ or $r = r_2$, where

$$r_1 = 2\frac{\sqrt{\Delta_1} - 3a(m-a)}{8a^2 - 8am + m^2} = \frac{2a(m-a)}{\sqrt{\Delta_1} + 3a(m-a)}, \qquad r_2 = -2\frac{\sqrt{\Delta_1} + 3a(m-a)}{8a^2 - 8am + m^2}.$$

The second expression for r_1 is obtained by multiplying the numerator and the denominator of r_1 by the conjugate expression, $\sqrt{\Delta_1} + 3a(m-a)$, of the numerator, or by using the relation $r_1 r_2 = \frac{-4a(m-a)}{8a^2 - 8am + m^2}$. Hence $r_1 = r_* > 0$, is the value given in the proposition. Note that $r_2 > 0$ for $8a^2 - 8am + m^2 < 0$, which occurs if and only if

$$\frac{2-\sqrt{2}}{4}m < a < \frac{2+\sqrt{2}}{4}m.$$

From the relation $\Delta = b^2 - 4c$, it is seen that for all $a \in (0, m)$, we have

$$\Delta \geq -4a(m-a)(r^2 - 3r + 1)$$

and the equality holds if and only if $a = m/2$. Therefore, for all $a \in (0, m)$, we have

$$0 < r_1 \leq \frac{3-\sqrt{5}}{2}, \quad \text{and the equality holds only for} \quad a = m/2.$$

This proves the condition on r_* given in the proposition. On the other hand, we have:

$$\begin{aligned} &\text{for all } a \in \left(0, \tfrac{2-\sqrt{2}}{4}m\right) \cup \left(\tfrac{2+\sqrt{2}}{4}m, m\right), && r_2 < 0, \\ &\text{for all } a \in \left(\tfrac{2-\sqrt{2}}{4}m, \tfrac{2+\sqrt{2}}{4}m\right), && r_2 \geq \tfrac{3-\sqrt{5}}{2}. \end{aligned}$$

In the first case, $\Delta > 0$ for $r < r_2$ or $r > r_1$, and in the second case, $\Delta > 0$ for $r_1 < r < r_2$. Therefore, for all $a \in (0, m)$, we have $\Delta > 0$ for all $r \in (r_*, 1/2)$. From these results on the signs of $b = d_1 + d_2$, $c = d_1 d_1$ and Δ we deduce the following results. Assume that $0 < a < m/2$.

- If $0 < r < r_*$ then $\Delta < 0$, i.e. d_1 and d_2 are complex conjugate. There is no intersection point.
- If $r = r_*$, then $\Delta = 0$, i.e. $d_1 = d_2 = \frac{r_*(m-2a)}{2} > 0$. $Q_1 = Q_2$ is the unique intersection point.
- If $r_* < r < \frac{3-\sqrt{5}}{2}$, then $\Delta > 0$, $d_1 + d_2 > 0$ and $d_1 d_2 > 0$, i.e. $0 < d_2 < d_1$. Q_1 and Q_2 are the two intersection points.
- If $r = \frac{3-\sqrt{5}}{2}$, then $\Delta > 0$, $d_1 + d_2 > 0$ and $d_1 d_2 = 0$, i.e. $0 = d_2 < d_1$. Q_1 is the unique intersection point.
- If $\frac{3-\sqrt{5}}{2} < r < \frac{1}{2}$, then $\Delta > 0$ and $d_1 d_2 < 0$, i.e. $d_2 < 0 < d_1$. Q_1 is the unique intersection point.

Similarly we see that when $m/2 \leq a < m$, if $0 < r \leq \frac{3-\sqrt{5}}{2}$, then there is no intersection point and, if $\frac{3-\sqrt{5}}{2} < r < \frac{1}{2}$, then Q_1 is the unique intersection point.

D.4. **Proof of Proposition 13.** In the Monod case one has

$$\lambda(D+a) = \tfrac{K(D+a)}{m-D-a}, \qquad S_1^* = \lambda\left(\tfrac{D}{r} + a\right) = \tfrac{K(D+ra)}{mr-D-ra}.$$

Thus, one must have $mr > D + ra$, which also gives $m > D + a$. The equation $f(S_2) = h_2(S_2)$ is equivalent to an algebraic quadratic equation. Therefore this equation has at most two real solutions. We will show that this equation actually has exactly two positive solutions. This result is obviously in agreement with the result of Lemma 2, which states that, for any increasing growth function, the equation $f(S_2) = h_2(S_2)$ has at least two positive solutions, and with Assumption 2, satisfied by a Monod function, which states that there are only two solutions. The algebraic quadratic equation resulting from the equation $f(S_2) = h_2(S_2)$ is

$$c_2 S_2^2 - c_1 S_2 + c_0 = 0$$

with c_i, $i = 0, 1, 2$ defined by

$$\begin{array}{rcl} c_2 & := & (m - (D+a))(mr - (D+ra))(Dm - a^2 r + amr), \\ c_1 & := & K(b_2 m^2 - b_1 m + b_0), \\ c_0 & := & K^2 a^2 r (D+ra)(m - (D+a)), \end{array} \tag{51}$$

where b_i, $i = 0, 1, 2$ are given by

$$\begin{array}{rcl} b_2 & := & r(2Da + D^2 + 2a^2 r), \\ b_1 & := & 2raD^2 + 4rDa^2 + D^3 + 2r^2 a^2 D + aD^2 + 4r^2 a^3, \\ b_0 & := & 2a^2 r(D+a)(D+ra). \end{array} \tag{52}$$

Remark that c_2 and c_0 are positive because $mr > D + ra$ and $m > D + a$. In addition, remark that b_0, b_1 and b_2 are positive and $\frac{\partial c_1}{\partial m} = K(2b_2 m - b_1)$ is positive for all $m > b_2/2b_1$. This computation shows that

$$\tfrac{D}{r} + a - \tfrac{b_2}{2b_1} = \tfrac{5D^2 a + 3D^3 + 12Da^2 r + 4raD^2 + 8r^2 a^3 + 2r^2 a^2 D}{2r(2aD + D^2 + 2a^2 r)}.$$

is positive. Thus, c_1 as a function of m is increasing for all $m > D/r + a$. In addition,

$$c_1(D/r + a) = KaD^2(D/r - D + a(1-r))$$

is positive. Consequently, $c_1(m)$ is positive for all $m > D/r + a$.

On the other hand, one has

$$\Delta = c_1^2 - 4c_2 c_0 = D^2 K^2 m^2 \Delta_1(m), \quad \text{with} \quad \Delta_1(m) = v_2 m^2 - v_1 m + v_0, \tag{53}$$

where v_i, $i = 0, 1, 2$ are given by

$$\begin{array}{rcl} v_2 & := & r^2(4a^2 r + D^2 + 4aD), \\ v_1 & := & 2r(2Da^2 r^2 + 4a^3 r^2 + 2D^2 ar + 6Da^2 r + D^3 + 3D^2 a), \\ v_0 & := & (D+a)(4a^3 r^3 + 8Da^2 r^2 + 4D^2 ar + D^3 + D^2 a). \end{array} \tag{54}$$

The discriminant of Δ_1 is given by

$$\Delta_0 = (v_1/2)^2 - v_2 v_0 = 4D^2 r^2 a^3 (-1+r)^3 (D + ra)$$

and is negative. As v_1 is positive we deduce that $\Delta_1(m) > 0$, for any m. Consequently, equation $f(S_2) = h_2(S_2)$ admits two positive solutions $S_2^1(D)$ and $S_2^2(D)$, such that $0 < S_2^1(D) < S_2^2(D) < \sigma$. The explicit expressions of these two solutions are

$$S_2^1(D,r) = \frac{c_1 - \sqrt{\Delta}}{2c_2}, \quad S_2^2(D,r) = \frac{c_1 + \sqrt{\Delta}}{2c_2}$$

where c_1 and c_2 are defined in (51) and Δ is given by (53). We deduce the expressions of $p_2^1(D,r)$ and $p_2^2(D,r)$ from $S_2^1(D,r)$ and $S_2^2(D,r)$ by using (29).

References

[1] M. Dali-Youcef, J. Harmand, A. Rapaport, T. Sari. Some non-intuitive properties of serial chemostats with and without mortality. 2021. hal-03404740

[2] M. Dali Youcef, A. Rapaport and T. Sari, Study of performance criteria of serial configuration of two chemostats, *Math. Biosci. Eng.*, 17(6) (2020), 6278-6309.

[3] M. Dali-Youcef, A. Rapaport and T. Sari, Performances study criteria of two interconnected chemostats with mortality, hal-03318978

[4] C. D. de Gooijer, W. A. M. Bakker Wilfried, H. H. Beeftink, J. Tramper, Bioreactors in series: An overview of design procedures and practical applications, *Enzyme Microb. Tech.*, 18 (1996), 202–219.

[5] I. Haidar, A. Rapaport, A. and F. Gérard, Effects of spatial structure and diffusion on the performances of the chemostat. Mathematical Bioscience and Engineering. 8(4) (2011), 953–971.

[6] J. Harmand, C. Lobry, A. Rapaport and T. Sari, *The Chemostat: Mathematical Theory of Microorganism Cultures*, John Wiley & Sons, Chemical Engineering Series, 2017.

[7] J. Harmand, A. Rapaport and A. Trofino, Optimal design of two interconnected bioreactors–some new results. AIChE J. 49(6) (1999), 1433–1450.

[8] D.R. Herbert, R. Elsworth and R.C. Telling, The continuous culture of bacteria: a theoretical and experimental study. *J. Gen. Microbiol* 14 (1956), 601-622.

[9] G. Hill, C. Robinson, Minimum tank volumes for CFST bioreactors in series, *Can. J. Chem. Eng.*, 67 (1989), 818–824.

[10] M. Nelson and H. Sidhu, Evaluating the performance of a cascade of two bioreactors. Chem. Eng. Sci. 61 (2006), 3159–3166.

[11] S. Pavlou, Computing operating diagrams of bioreactors, J. Biotechnol., 71 (1999), 7–16, 10.1016/s0168-1656(99)00011-5

[12] M. Polihronakis, L. Petrou and A. Deligiannis, Parameter adaptive control techniques for anaerobic digesters—real-life experiments, *Elsevier, Computers & chemical engineering*, 17(12) (1993), 1167-1179.

[13] A. Rapaport, Some non-intuitive properties of simple extensions of the chemostat model, *Ecol. Complexity*, Elsevier, 34 (2018), 111–118.

[14] P. Renard, D. Dochain, G. Bastin, H. Naveau and E. J. Nyns, Adaptive control of anaerobic digestion processes – a pilot-Scale application. *Biotechnology and Bioengineering*, Vol. 31, Pp. 287-294 (1988).

[15] E. Scuras, A. Jobbagy, L. Grady, Optimization of activated sludge reactor configuration: kinetic considerations, *Water Res.*, 35 (2001), 4277–4284.

[16] H. Smith and P. Waltman, The Theory of the Chemostat, Dynamics of Microbial Competition. Cambridge University Press, 1995.

[17] B. Tang, Mathematical investigations of growth of microorganisms in the gradostat, *J. Math. Biol.*, 23 (1986), 319–339.

[18] J. Zambrano, and B. Carlsson, Optimizing zone volumes in bioreactors described by Monod and Contois growth kinetics *Proc. IWA World Water Congress : 2014*.

MISTEA, Univ Montpellier, INRAE, Institut Agro, Montpellier, France
Current address: Avignon Université, Laboratoire de Mathématiques d'Avignon, Avignon, France
Email address: Manel.Dali-Youcef@inrae.fr

ITAP, Univ Montpellier, INRAE, Institut Agro, Montpellier, France
Email address: Tewfik.Sari@inrae.fr